

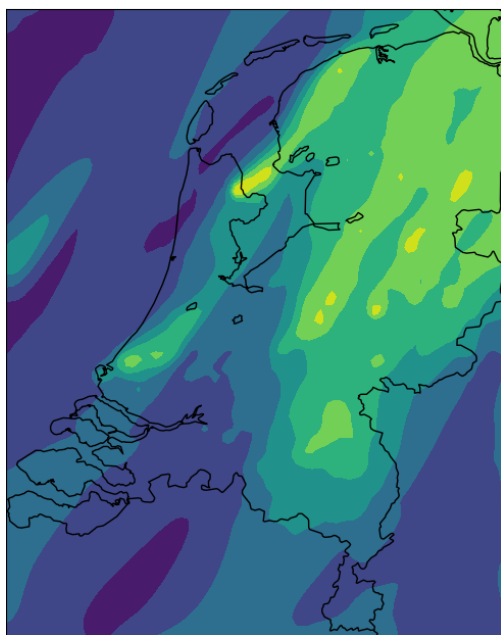
UTRECHT UNIVERSITY

INSTITUTE FOR MARINE AND ATMOSPHERIC RESEARCH

CLIMATE PHYSICS

MASTER THESIS

**High resolution simulations of methane
concentrations in the Netherlands using
WRF-Chem**



Author

I.T.B. QUAX

Supervisors

Prof.dr.ir. G.J.M. VELDERS

Prof.dr. T. RÖCKMANN

October 1, 2020

Abstract

Enhanced methane (CH₄) concentrations account for 23% of the anthropogenic radiative forcing. This study seeks to contribute to the insights in the methane emissions in the Netherlands. In this study the WRF-Chem model is used to conduct simulations of CH₄ concentrations in the Netherlands. The aim of this study is to test the quality of high resolution simulations of methane concentration. An emission inventory with a resolution of 1 km x 1 km is used as input in the WRF-Chem model. High resolution simulations of the methane concentration in 2017 are conducted with a grid size of 3 km x 3 km, on the domain of the Netherlands. The emissions from the inventory were used as input for 13 individual tracers, one for every emission subgroup in the inventory. To test the quality of these simulations, the results are compared with *in situ* measurements of methane concentration from measurement sites at Lutjewad and Cabauw. The analysis showed an underestimation of the simulated CH₄ concentration compared to the observed CH₄ concentration during peak events. This underestimation is probably caused by using the average CH₄ emissions over the volume of a 3 km x 3 km grid as input. For this reason local plume emissions are less dense in the simulations. The observed diurnal range in the CH₄ concentrations is 3 to 4 times larger at Lutjewad and Cabauw than the diurnal range in the simulated CH₄ concentration during summer. The opposite would be expected from the daytime nighttime ratio of the boundary layer height, which is larger in the simulations than in the observations. Furthermore, implementing diurnal variability in several smaller emission sources did not improve the diurnal range in the simulated methane concentration. The WRF-Chem simulations correctly reproduce the wind direction for which the excess CH₄ concentration is highest in Lutjewad. The relative magnitude of the excess CH₄ concentration for this wind direction is underestimated in the simulations. This can be caused by the poor representation of the diffusion of plume emission in the simulation. Another cause could be underestimated methane emissions around the measurement sites. The WRF-Chem simulations showed underestimations in the magnitude of the variability of methane concentration on several timescales. In order to increase the accuracy of the WRF-Chem simulations of CH₄ concentrations, further research is need to gain insight into the causes of the differences in the variability of the simulated and observed CH₄ concentrations.

Acknowledgements

First of all I would like to thank Friedemann Reum for his extensive help during my master research project. His help played a crucial role in preparing the WRF-Chem model and the simulations conducted in this study. Sebastian Wolff also played an important role in helping me to prepare the simulations, for which I am very grateful. Furthermore, I am very grateful to Guus Velders for supervising my master research project. His support and critical view throughout my master research project gave me new insights in conducting and interpreting the research and results of the study. I would like to thank Huilin Chen and Bert Scheeren from the Rijksuniversiteit Groningen as well, for providing me with the methane measurement data of Lutjewad. I would like to thank Arnoud Frumau and Arjan Hensen from the Netherlands Organisation for applied scientific research (TNO), for providing me with the methane measurement data of Cabauw. I am also grateful to Marijn de Haij from the Koninklijk Nederlands Meteorologisch Instituut (KNMI) for providing me with the boundary layer height data from Cabauw and Eelde.

Contents

1	Introduction	5
1.1	Research objectives	10
2	Method	11
2.1	The WRF-Chem model	11
2.2	Simulation area	12
2.3	Model setup	13
2.4	Emission data	14
2.4.1	National emissions from RIVM	14
2.4.2	European emissions from EDGAR	14
2.5	Methane measurement data	15
2.6	Boundary layer height	15
3	Results	17
3.1	Observation and WRF-Chem simulations compared	18
3.1.1	Year averaged	18
3.1.2	Methane concentration per month	24
3.2	Diurnal cycle	26
3.2.1	Methane concentration	26
3.2.2	Boundary layer height	30
3.3	Influence of wind direction on tracers concentration	32
3.3.1	Simulated wind direction compared with observations	32
3.3.2	Methane concentration depending on wind direction	36
3.4	Qualitative error analysis	41
4	Discussion	42
4.1	WRF-Chem simulation and <i>in situ</i> observations compared	42
4.1.1	Seasonal variability	42
4.1.2	Peak events	42
4.1.3	Correlation per year	44
4.1.4	Correlation per month	45
4.2	Diurnal cycle of methane concentration	45
4.2.1	Boundary layer height	46
4.3	Effect of wind direction on tracer concentration	47
4.4	Limitations	48
4.4.1	The WRF-Chem model	48

4.4.2	Input data	49
4.4.3	Measurement data	49
4.5	Recommendations for further research	50
5	Conclusion	50
6	References	53
7	Appendix	58
7.1	Tables of tracers	58
7.2	Maps of CH ₄ emissions per tracer in the Netherlands	61
7.3	WRF namelist settings	74

1 Introduction

In the present day world, the changing climate is a major threat and counteracting it is an unprecedented challenge. Anthropogenic emissions of greenhouse gasses are the main cause of global warming. There are several greenhouse gasses, of which carbon dioxide is the most important one. Methane (CH_4) is the second most important greenhouse gas. The global atmospheric concentration of methane has risen from 722 parts per billion (ppb) in 1750 to 1876 ppb in 2020 (Etheridge et al., 1998, NOAA Research, US Department of Commerce, 2020). This is approximately 2.6 times larger than the pre-industrial methane concentration and accounts for 23% of the anthropogenic radiative forcing (Saunio et al., 2020). The main sources of the increase in atmospheric methane in the past centuries are emissions from agriculture, i.e. cattle and rice paddies, and fossil fuel exploitation (Kirschke et al., 2013). Methane has a relatively short lifetime in the atmosphere, compared to carbon dioxide. The lifetime of methane is about 9 years and the main sink is oxidation with the OH radical (Lelieveld et al., 2016).

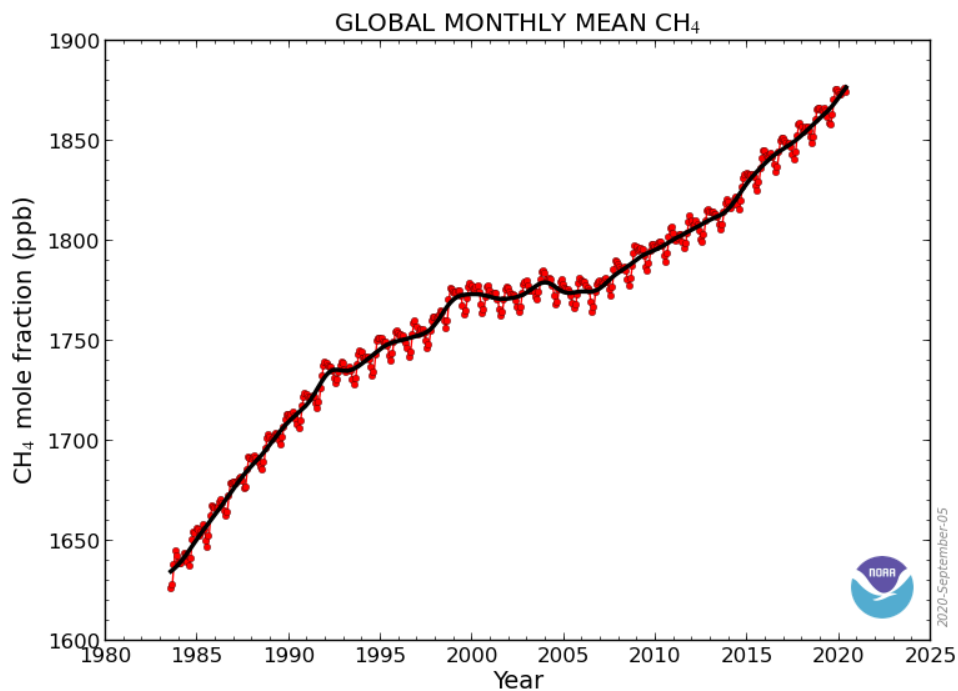


Figure 1: Global CH_4 concentration for 1983-2020. The black lines shows the yearly average CH_4 concentration. The red dots are the monthly average CH_4 concentrations. This global average CH_4 concentration is derived from a network of sampling sites (NOAA Research, US Department of Commerce, 2020)

The increase of CH_4 has not been continuous in the past decades, see figure 1. Until the 1990s the annual methane increase was about 12 ppb/year. From 1990 to 2000 the trend in methane concentration leveled off. From 2000 to 2007 the global CH_4 level stabilized and seemed to have reached a new steady state with almost no increase during that period. However, from 2007 onward, the global CH_4 level started

increasing again. In 2014 the global annual increase in CH₄ reached more than 10 ppb/year again (Kirschke et al., 2013). The cause of this temporary stabilization is still debated. Several causes have been addressed and investigated. One of the possible causes is the reduction of anthropogenic emissions from fossil fuel exploitation in countries of the former Soviet Union (Chen and Prinn, 2006, Simpson et al., 2012, Savolainen et al., 2009, Dlugokencky et al., 2003). Another reason that was suggested is the decreasing of wetland emissions (Bousquet et al., 2006, Chen and Prinn, 2006). A third cause for the decline of growth rates of CH₄ concentration is the reduced emissions from rice paddies due to changes in agricultural practices (Kai et al., 2011).

In the past decades, the main focus of climate change mitigation was on reducing CO₂ emissions. Attention for reducing methane emissions was sparse. The last decade the attention for reducing methane emission is rising and more effort will be put in reducing methane emissions. For example, this recently resulted in more focus of the European Green Deal on reducing methane emission (European Commission, 2020a) Due to the short lifetime of methane and the strong global warming potential (GWP) being much larger than carbon dioxide, reducing methane has a large potential of tempering global warming in the near future. In a time span of 100 years 1 kilogram of CH₄ is 28 times more potent of absorbing longwave radiation from the earth surface than 1 kilogram of CO₂. During the first 20 years, CH₄ is even 85 times stronger in warming the globe than CO₂ is (Myhre et al., 2013).

Enhanced methane concentrations in the atmosphere have additional negative effects. Methane is an important precursor gas for tropospheric ozone, which is also a greenhouse gas and has adverse effects for human health, as well as for animals, plants and materials. This is especially problematic in areas with high NO_x concentrations, such as urban areas (Lelieveld et al., 2016).

The most important natural source of methane are wetlands (Bridgham et al., 2013, Walter and Heimann, 2000). However, due to land-use change and water management, wetland emission can be enhanced by human activity (Conrad, 2002, Bachelet and Neue, 1993). Other important anthropogenic sources of methane are emissions from livestock, landfills, fossil fuel exploitation and distribution, traffic and energy production. Due to the large implications of methane emissions, it is important to gain more insight into the sources and sinks of methane and their magnitudes.

In the Netherlands, intensive livestock farming and the large wetland areas cause local increases in the methane concentration in the atmosphere above the Netherlands. The methane emission of the Netherlands is approximately 4% of the total CH₄ emission by the European Union (EU), while the Netherlands covers less than 1% of the total land surface of the EU. (European Commission, 2020b). Agriculture, in particular cattle, is the largest anthropogenic source of methane in the Netherlands. This is mainly caused by the enteric fermentation of plant material in the stomachs of cows and management of manure (RIVM, 2019). The Netherlands is the focus area of this study. Different sources play a main role in different parts of the country. As mentioned, agriculture is the most important source in the Netherlands with 69% of the total methane emission in the Netherlands (RIVM, 2019). Figure 2 shows the CH₄ emissions of the three largest

methane sources in the Netherlands. These emissions from cattle are mainly concentrated in the rural areas, especially the east part of the province of Noord-Brabant and the north part of the province of Limburg, the eastern part of the Netherlands and the province of Friesland. The second largest source in the Netherlands is waste disposal in landfills. Although the emissions by this source are strongly decreased in the past decades, waste disposal still accounts for 14% of the methane emission in the Netherlands, see figure 2. These landfills are located all around the country. Other important sources are the cogeneration engines, which are mainly used in greenhouses. Emissions from these engines accounts for 5% of the total methane emissions in the Netherlands and is highly concentrated in the small Westland area, located in the densely populated Randstad (Ministerie van Infrastructuur en Waterstaat, 2017). Furthermore, CH₄ emissions from traffic especially play a role in the urban area in the west of the Netherlands. The Groninger gas field is a small, but maybe underestimated source located in the north of the Netherlands (Yacovitch et al., 2018). The different sources and their magnitudes are shown in table 1. The total anthropogenic methane emission per 5 x 5 km in The Netherlands for 2017 is shown in figure 3.

Emissie methaan (CH₄) per sector

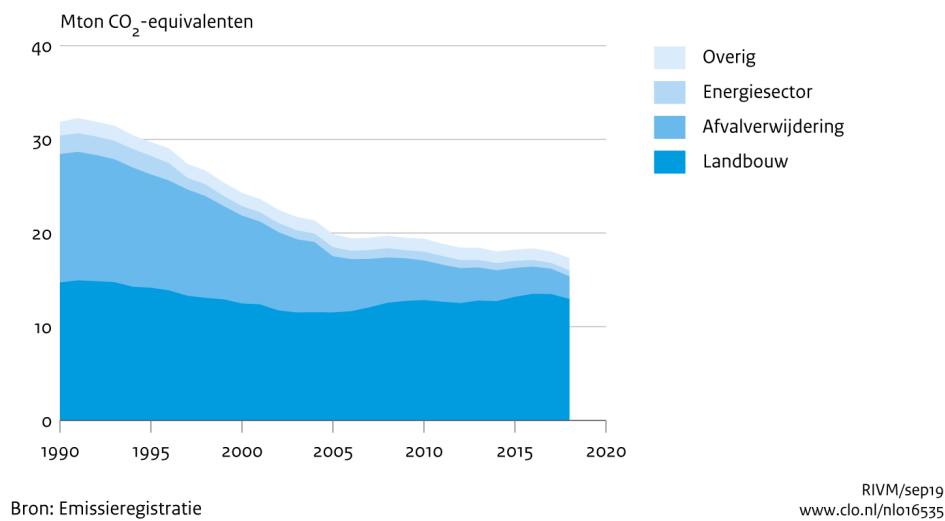


Figure 2: Methane emissions in the Netherlands from agriculture, waste, the energy sector and other sources in Mtons CO₂ equivalent per year, for the period 1990-2018 (Compendium, voor de Leefomgeving, 2020)

In the Netherlands detailed estimates are made for the most important greenhouse gases from 1990 onward every 5 year, and from 2015 on these calculations are published yearly by the Rijksinstituut voor Volksgezondheid en Milieu (RIVM) RIVM, Emissieregistratie, 2020. These calculated emissions are based on measured emissions from individual sources, such as a cow or a car, which are consequently extrapolated for all cars and cows etc. in the Netherlands (RIVM, 2019). These emission calculations give a very detailed understanding of all sources located in the Netherlands and their magnitudes. However, these

emissions are theoretical and continuous large scale measurements to verify these calculations are sparse. Performing greenhouse gas concentration simulations with the use of a model can play an important role in gaining insight in the quality of these emission calculations. Therefore, this study focuses on testing the accuracy with which this RIVM emission inventory represents the actual methane emissions in the Netherlands. This emission inventory is made with a high resolution of 1 km × 1 km. Figure 3 shows a map of the CH₄ emission data from this RIVM emission inventory.

In order to achieve this, the high resolution RIVM emission inventory of methane in the Netherlands is used as input in a weather forecast model coupled with a chemistry model, WRF-Chem (Skamarock et al., 2008). With the use of this model, methane concentrations in the atmosphere above the Netherlands are simulated. The results of this simulation are compared with available continuous data from two measurement sites in the Netherlands, Lutjewad and Cabauw. To make a meaningful comparison of the simulations with the measurements, the variation in CH₄ concentration of both simulations and measurements are compared. This comparison is made for variations on a diurnal, monthly and full year timescale. No diurnal or seasonal variation on the emissions in this emission inventory is reported by the RIVM. However, it is expected there is some diurnal and seasonal cycle in the methane emissions of some sources, for example because of less traffic at night and more energy use in wintertime (Bultjes et al., 2003). This is another aspect that can be tested with the simulations in this study. To investigate the diurnal variability in CH₄ emissions, a correct reproduction of the diurnal variability in CH₄ concentration by WRF-Chem is needed. The diurnal variability is mainly driven by the diurnal cycle in the planetary boundary layer height, or just boundary layer height (BLH). This effect is further explained in section 2.3 and investigated in the analysis of this study.

The emission inventory consists of yearly emission for 13 different emission groups (see table 1). Instead of looking at the total emission of all sources, these 13 emission groups can also be simulated individually in the WRF-Chem model. This can provide insight in the contribution of these individual emission groups to the concentration at the locations of the measurements. Because a different set of emission sources is located around the measurement sites of Lutjewad and Cabauw, it is expected that the wind direction has an influence on the concentration contribution of an emission group, at the measurement sites. This contribution is the so called excess concentration of a tracer. This is the residue of the concentration after subtraction of the background concentration.

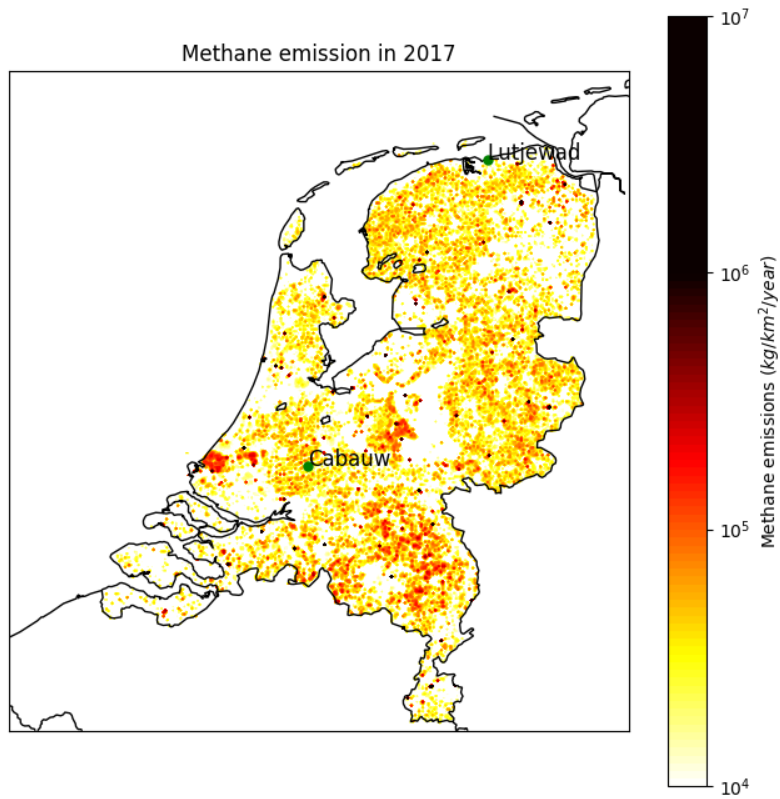


Figure 3: The total methane emissions in the Netherlands in 2017. Note that the color scale starts at 10^4 kg/km²/year. Emissions above 10^6 kg/km²/year are indicated with the color black, for better visibility (through the contrast).

Table 1: Methane emission of the Netherlands in 2017 per sector in tons/yr. The last column shows the percentage of the total CH₄ emission of the Netherlands. (Source: RIVM, Emissieregistratie, 2020)

Source	CH ₄ emission tons/yr	Percentage of total
Agriculture	539450	69.33%
Waste	111571	14.34%
Nature	70000	9.00%
Energy	21913	2.82%
Consumers	17407	2.24%
Waste water	7985.5	1.03%
Traffic and Transport	2806.7	0.36%
Trade and Government	1845.6	0.24%
Other Industry	1763.7	0.23%
Water purification	1724.2	0.22%
Chemical Industry	1119.1	0.14%
Refineries	405.5	0.05%
Construction	76.7	0.01%
Total	778100	100.00%

1.1 Research objectives

This thesis will focus on simulating methane concentrations in the Netherlands for the period of the full year 2017. The main objective is to conduct high resolution modelling experiments of methane concentrations with the use of a high resolution emission inventory and to evaluate the quality of these simulations by comparison with the available *in situ* measurements data. The following questions will be addressed and answered to reach the objective of this study:

- Can the observed methane concentration in Lutjewad and Cabauw be reproduced by model simulations with the use of a high resolution methane emission inventory as input in the WRF-Chem model?
- How well does the simulation without diurnal or season cycle in the emission correspond to the measurements in Lutjewad and Cabauw?
- Can the implementation of diurnal cycles on the emission improve the correspondence in diurnal trend between simulations and measurements, and if not can other causes be addressed?
- Does the wind direction have impact on the excess concentration of the tracers detected at the measurement locations?

2 Method

2.1 The WRF-Chem model

For the simulations of methane concentrations in the Netherlands in this study, the Weather Research and Forecasting model coupled with Chemistry (WRF-Chem) is used (Skamarock et al., 2008). One of the applications of the WRF model is conducting research on weather predictions and atmospheric dynamical processes. This WRF model is coupled with a chemistry model to make it suitable for research on chemical processes in the atmosphere. Emissions of gasses and aerosols can be used as input to simulate the concentrations in the atmosphere. Besides using it for simulating chemical active gasses, this model is also suitable for simulations of chemically inactive gasses, so called passive tracers. This option for passive tracers makes this WRF-Chem model very suitable for simulations of greenhouse gas concentrations which have a lifetime much longer than the simulation period, such as CO₂ and CH₄ (Beck et al., 2011). The WRF-Chem model uses meteorological data for simulating the dynamics and distribution of emitted gasses in the atmosphere. In figure 4 a flowchart is shown indicating the main processes involved in conducting a WRF-Chem simulation. The preparation of the model simulation is conducted with the WRF pre-processing system (WPS). The input terrestrial data and meteorological data are prepared for the simulation domains and period with the use of this WPS. The meteorological data is prepared on time intervals of 6 hours. This pre-processed data is used as input in the WRF-Chem model. The pre-processed meteorological data is used to update the meteorological conditions in the simulations every 6 hours. The initial conditions in both domains and boundary conditions at the borders of the outer domain, are obtained from the Copernicus Atmospheric Monitoring Service (CAMS). This CAMS data is used as input at every time step of the simulations. Furthermore, the emission data from the RIVM and EDGAR emission inventories are used as input for the WRF-Chem model. After all this data is prepared as input, the simulations are conducted. The output of the WRF-Chem simulations is subsequently visualized and analyzed with the use of Python.

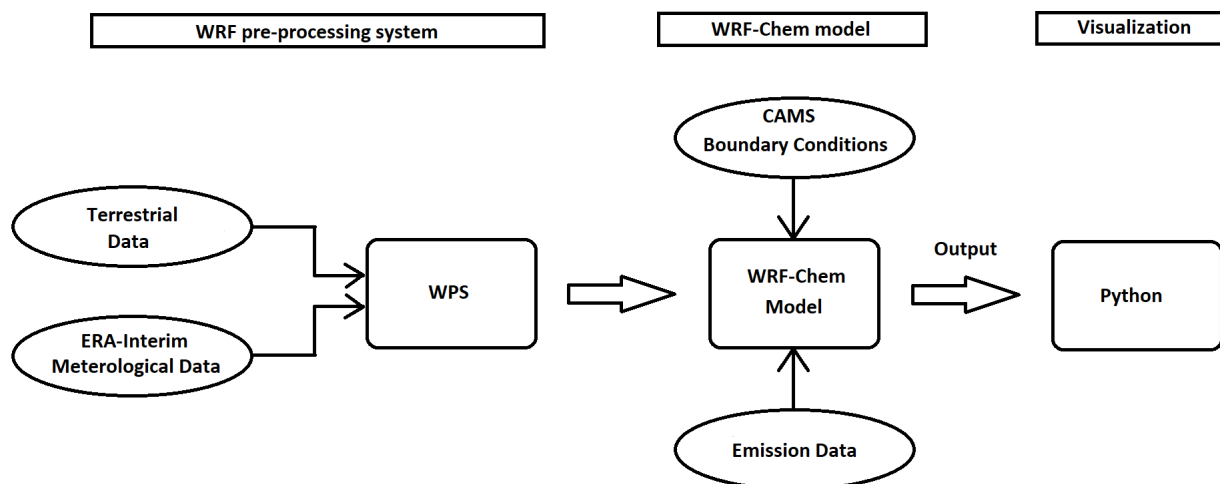


Figure 4: Flowchart of the main processes involved in preparing and conducting simulations with the WRF-Chem model (Figure from Park et al., 2015, adjusted by Ivo Quax).

In the past years several studies have been conducted with the use of this WRF-Chem model using passive tracers. Kort et al. (2014) published a study in which WRF-Chem simulations were used to show the underestimation by the EDGAR emission inventory of the CH₄ emissions in the Four Corner region in the U.S.. Satellite and *in situ* measurements were compared with WRF-Chem simulation output to test the accuracy of this EDGAR emission inventory (Kort et al., 2014). Another study (Beck et al., 2013) used the WRF-Chem model to test different wetland inundation maps of the Amazon region on reproducing the wetland CH₄ emission in this area. Recently, a study (Reum et al., 2020) showed how WRF-Chem, coupled with the CTDas, can be used to estimate greenhouse gas fluxes on various spatial scales (Reum et al., 2020). This selection of studies using WRF-Chem shows that this model is a suitable candidate to use for research on greenhouse gas emissions.

2.2 Simulation area

The region of interest for this study is the area of the Netherlands. High resolution simulations will be conducted on the inner domain shown in figure 5. This area is chosen because of the availability of a high resolution methane emission inventory by the RIVM. This, together with the fact that the Netherlands has a relatively high atmospheric CH₄ concentration, makes this an important area to study (Villani et al., 2010). The *in situ* methane measurements used in this study are the only two continuous measurement sites on CH₄ concentration in the Netherlands, Lutjewad and Cabauw. These measurement locations are highlighted in figure 5. Lutjewad is located in the sparsely populated north of the Netherlands. The measurement site is at the coast of the Wadden sea, which stretches out at the north of Lutjewad. To the south, Lutjewad is surrounded by agricultural land. Furthermore, this site is in the middle of the Groningen gas field production area in which large amount of natural gas are extracted. Cabauw is located 200 kilome-

tres to the south-west of Lutjewad. The measurement site is situated in the middle of agricultural land, but is also close to large cities such as Utrecht, Den Haag, Rotterdam and Amsterdam. This measurement site is within 50 kilometres of an area of intensive cattle production in Noord-Brabant. For this reason it is expected that many different sources play an important role here, depending of the wind direction.

The simulations will be conducted for the year 2017, from the 1st of January to 31st of December. The inner domain shown in figure covers an area of approximately 260x330 km. The aim was to use a resolution of 1x1 km for this domain. However, this turned out to be unfeasible, because very long computer running time would be necessary. Therefore, a resolution of 3x3 km is therefore chosen for the inner domain. To optimize boundary values and gain insight in the methane emission surrounding the Netherlands, an outer domain is chosen with a size of 900x900 km and resolution of 9 x 9 km.



Figure 5: On the left panel the outer simulation domain (D1) of 900 x 900 km together with the nested simulation domain (D2) of 260 km in longitudinal direction and 330 km in latitudinal direction are shown. The locations of the measurement sites are indicated in the right panel.

2.3 Model setup

For the atmospheric simulations in this study the WRF-Chem model version 4.1.1 is used. For pre-processing the WPS model version 4.1 is used. This model has options for the simulation of passive tracers with input emission data. Passive tracers are gasses that are considered chemically non-reactive. For methane this assumption is valid for the simulation period for two reasons. First of all, the lifetime of methane in the atmosphere is about 9 years, thus in 1 year only a small part will be removed by chemical reaction with OH. Furthermore, the simulation domains are relatively small, therefore the emitted methane stays only for a short period in the domains, before it is transported out of the domain by the wind.

To find the right model setup, intensive cooperation has been conducted with Friedemann Reum from Netherlands Institute for Space Research (SRON) institute and Sebastian Wolff from the Deutsches Zentrum

für Luft- und Raumfahrt (DLR). The working settings that have been used for this study were based on their experience. The complete list of settings used for the WRF-Chem model in this study can be found in the appendix (section 7). For the meteorology input data the ERA-Interim reanalysis data from 2017 is used. This data has 60 pressure levels and 4 soil levels with a resolution of approximately 80x80 km with a time interval of 6 hours (ECMWF, 2020b). For the initial and boundary conditions of the methane concentration in these simulations, data from the Copernicus Atmospheric Monitoring Service (CAMS) is used (ECMWF, 2020a). This data is based on satellite observations combined with ground measurements.

2.4 Emission data

2.4.1 National emissions from RIVM

The input data used for the emissions in the nested domain covering the Netherlands is provided by the RIVM (RIVM, Emissieregistratie, 2020). This data is based on the present knowledge about individual sources and the number of these sources distributed throughout the Netherlands. The resolution of this emission data is 1km x 1km. The sources are categorized in 13 subgroups (see table 1). These 13 subgroups are simulated as 13 independent passive tracers. The provided data are total emissions per km² in 2017. The data is converted to mole/seconds to generate constant emission in the model for the full period of 2017. No information on daily or seasonal cycles is available from the RIVM. At first, simulations are conducted with the original RIVM data from the emission inventory. Because diurnal cycles are expected for some emission sources, a second run is conducted in which diurnal cycles are implemented for several emissions groups. These cycles are based on intensity of human activity throughout the day and are general for most greenhouse gasses. These cycles are based on a report of TNO (Bultjes et al., 2003). The multiplication factors for the diurnal cycles of all emission groups can be found in table 8 and 9 in the appendix. This emission data is written on the Dutch Rijksdriehoek coordinate system, which is a Cartesian coordinates system, meaning it uses the unit meter. The data is written at the location of the left lower corner of each grid. To use this data in WRF-Chem it has to be converted to another coordinates system, in this case a geographic coordinate system with unit degree. The RIVM data is given on a rectangular area of 556 km in north-south by 320 km in west-east direction. This rectangular area on a Cartesian system becomes a trapezium shape in a geographic coordinate system, which is wider on the north and narrower on the south. WRF-Chem can only deal with rectangular shapes in a geographic system. For this reason the RIVM data is spread out over a rectangular shape in which the south side has the same distance in degrees as the north side. This results in a deviation on the order of tenths of degrees in longitudinal direction.

2.4.2 European emissions from EDGAR

For the outer domain methane emission data of the Emission Database for Global Atmospheric Research (EDGAR) is used. The EDGAR database is a joint research project from the European Commission DG JRC

and the Netherlands Environmental Assessment Agency (European Commission, 2020b). This data has a resolution of 0.1×0.1 degrees, which corresponds to approximately 10×10 km. This methane emission data is categorized in 26 subgroups. These subgroups do not fully cover all subgroups of the RIVM data. Natural emissions are not provided by the EDGAR database. The EDGAR subgroups are divided over the 13 RIVM subgroups as shown in table 7 in the appendix. For the groups of the RIVM data that are not covered by the EDGAR data the corresponding tracers are implemented as having zero emission in the coarse domain. The most recent available emission data for methane in the EDGAR database is for the year 2015. The data from 2015 is used for the simulations of 2017 in this study. Differences in emissions between these years are assumed to be rather small.

2.5 Methane measurement data

The output data from the simulations is compared with continuous measurements of atmospheric CH_4 concentrations on two location in the Netherlands, Lutjewad ($53^\circ 24' \text{ N}$, $6^\circ 21' \text{ E}$) and Cabauw ($51^\circ 58' 16' \text{ N}$, $4^\circ 55' 36' \text{ E}$). In Lutjewad these measurements are conducted by the Centre of Isotopic Research (CIO) of the Rijksuniversiteit Groningen and for this study provided by Bert Scheeren (Rijksuniversiteit Groningen, 2020). The CH_4 measurements in Cabauw are conducted and monitored by the Netherlands Organisation for applied scientific research (TNO) and for this study provided by Arnoud Frumau. The concentrations are measured with the Picarro 2301 device (Fruman, 2016). The measurement height of CH_4 is 60 m above ground level. The datasets consist of hourly concentration data. The institutions, CIO and TNO, already marked all data points containing bad data. In both datasets these bad data points or data gaps were masked. Both datasets have gaps throughout 2017, some of them up to 14 days in a row. The masked data points are also masked in the simulation data and left out for the analysis in order to use only data at times that occur in both datasets.

2.6 Boundary layer height

The diurnal cycle in the boundary layer height plays an important role in the diurnal variability of the CH_4 concentration. The boundary layer is the lowest layer of the atmosphere which is influenced by earth surface processes. This layer is well mixed and varies between 200 m and 2 km depending the location, the season and the time of the day. Transport of gasses and particles from the boundary layer to the free atmosphere above it, is low. During daytime the boundary layer is turbulent due to buoyancy forces induced by heating of the earth surface. Gasses in this layer are well mixed when this layer is turbulent. During nighttime the buoyancy force disappears due to the cooling of the earth surface. The boundary layer becomes stratified. Emissions from CH_4 sources not be captured in a much thinner layer during the night than during the day. For this reason nighttime CH_4 concentrations at the measuring height (60m) can become much higher during the night than during the day. The ratio between daytime and nighttime BLH

determines roughly the ratio between the daytime and nighttime excess CH₄ concentration (de Haij et al., 2017).

There are many different definitions for indicating the top of the boundary layer. Reliable measurements of the boundary layer height in 2017 are only available for Cabauw and not for Luttjewad. The measurements of the boundary layer height are conducted with the LIDAR (Ligth Detection and Ranging) method (de Haij et al., 2017). In this method the backscattering of a laser signal is used to determine the vertical gradient in tracer concentration. The boundary layer height is characterized by a strong vertical gradient in particle concentration. In the WRF-Chem simulations the Yonsei University (YSU) scheme is used for simulating the top on the boundary layer (Hong and Pan, 1996, Hong, 2010). This scheme is based on the Bulk Richardson Number (BRN). This BRN represents the generation of turbulence kinetic energy caused by wind shear. The top of the boundary layer is corresponds to a critical value of the BRN (Hong and Pan, 1996, Shi et al., 2020). With the use of this YSU scheme, the boundary layer height is determined with the use of several meteorological parameters.

3 Results

In the first part of this results section the CH₄ concentration output data of the simulation are shown. This data is compared with the observations in both Lutjewad and Cabauw. First, this is done for the full simulation period and, thereafter, per month. Next, the diurnal cycle in the CH₄ concentration is analyzed and simulation and observations are compared again. The first run is done without diurnal cycle in the emission. A second run is performed in which diurnal cycles are implemented in the emissions for several tracers. This second run is also compared with the observations to see whether the simulation output is improved. Furthermore, the boundary layer height of the simulation and observations are compared. In the final part of this results section, the wind direction and its influence on the excess methane concentrations induced by the individual tracers is determined.

Figure 6 shows as an example a map of the total simulated CH₄ concentration in the inner simulation domain on 11th of September 2017 at 3:00 p.m.. This map shows the high resolution of the simulation output. Local CH₄ concentration anomalies from areas with high CH₄ emissions are visible on the map. For example, a CH₄ plume from the Westland area is visible. Plumes from the east of Utrecht and the east of Brabant provinces are also shown on the map. The CH₄ plumes from these areas of high concentration stretch out towards the northeast. The measurement locations Lutjewad and Cabauw are indicated in figure 6. For the analysis discussed throughout this section, only the simulated data of the grids in which Lutjewad and Cabauw are located was used.

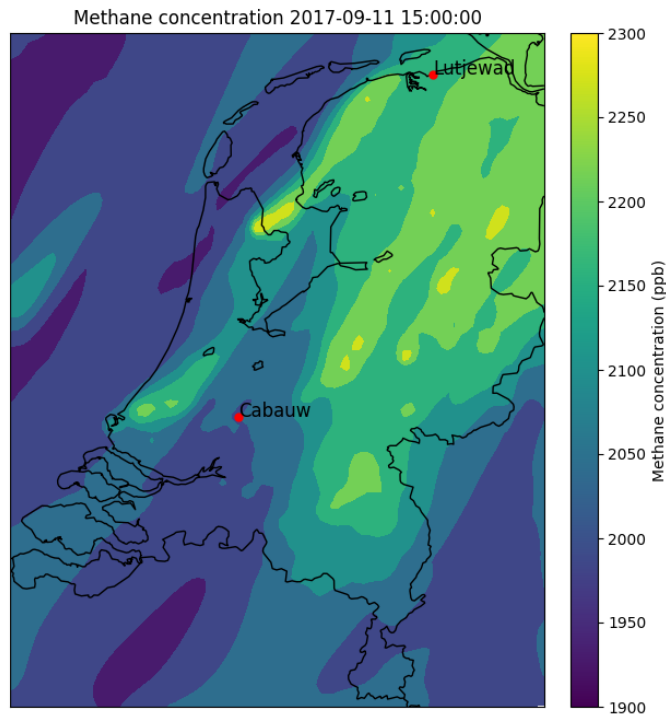


Figure 6: A map of the simulated CH₄ concentration in the inner simulation domain on 11th of September 2017 at 3:00 p.m.. The measurement locations Lutjewad and Cabauw are indicated on the map.

3.1 Observation and WRF-Chem simulations compared

3.1.1 Year averaged

The simulations are conducted for the year 2017. Every tracer represents a group of emission sources. In figure 7 the concentrations of the individual tracers in 2017 are plotted. The concentrations are made up by the emissions of the 13 different groups of sources, on top of the background concentration.

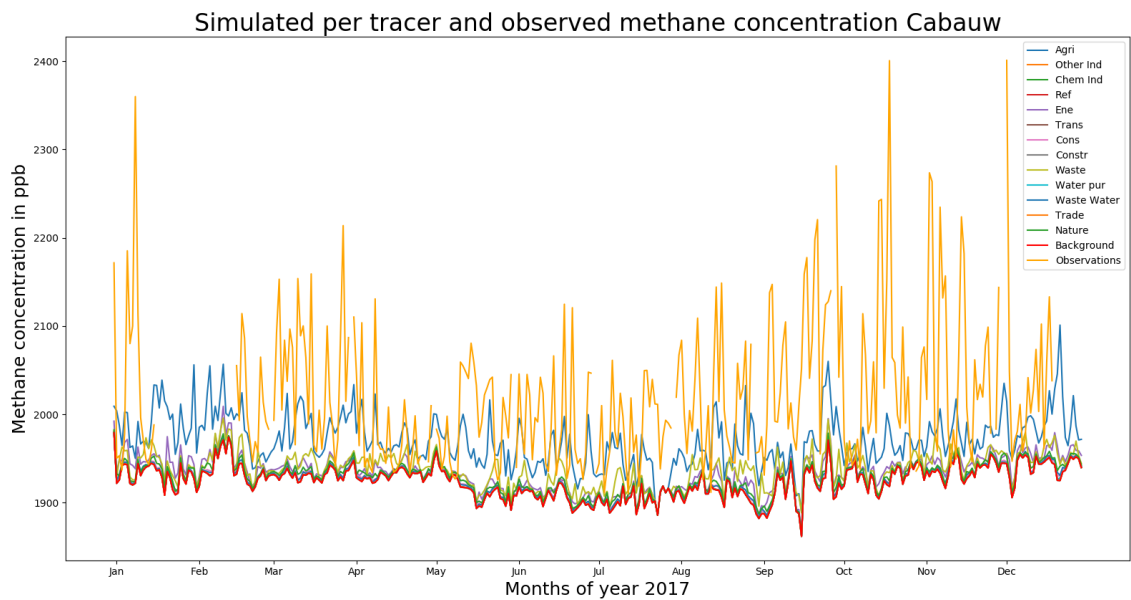
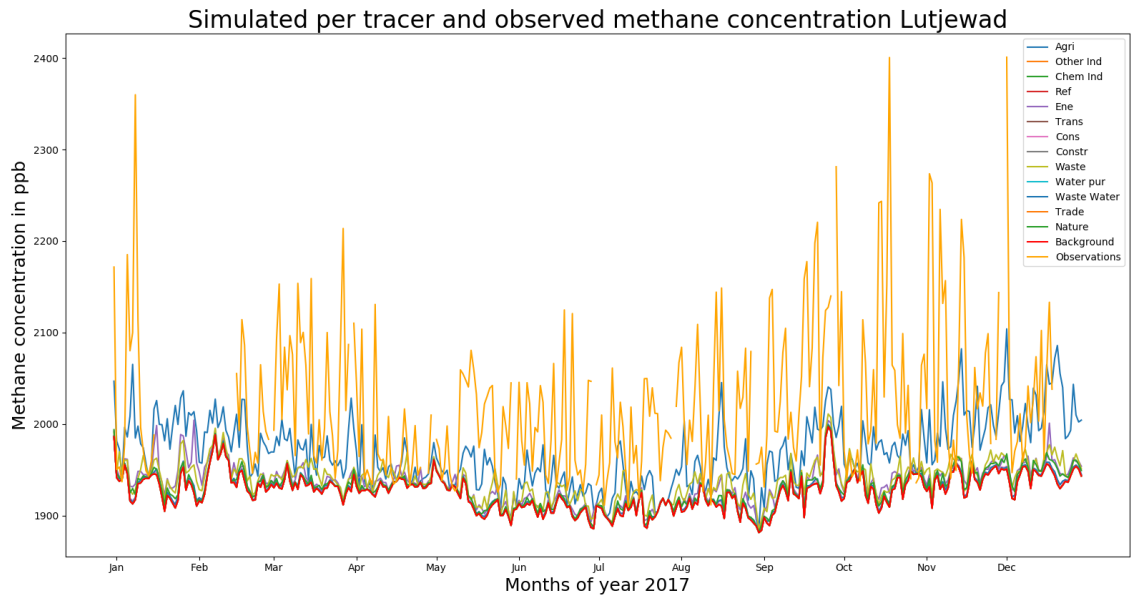


Figure 7: The simulated methane concentration per tracer and the observations (orange line) are shown above for Lutjewad (top) and Cabauw (bottom) for the year 2017. This is the original simulation output, thus in the plotted concentration of each tracer the background concentration is included. The tracer names in the legend are abbreviations of the names given in table 1.

In both Lutjewad and Cabauw large peaks are observed in the methane concentration in 2017. For short periods of time, concentrations of 2400 ppb are observed in both locations. Although the magnitudes of these peaks are not fully represented by the individual simulated tracers, many of these peaks in the obser-

vations do also occur in the individual tracers simulations. The tracer for agricultural emissions shows the highest concentration of all tracers, see the blue line in figure 7. The graphs demonstrate that the concentration of agricultural emissions seems to represent these peak events in the observations best. The second highest concentrations occur for the tracer representing the CH₄ emission from waste. The red line is the background concentration, i.e. the simulated concentration without any emissions in the simulation domains. The background concentration is determined by the boundary conditions of CH₄ concentrations implemented at the borders of the outer domain. The background shows, as expected, the lowest concentration of all tracers. Furthermore, the background concentration represents the observed peak events least well. The plots in figure 7 also show the gaps in the observed data. A limitation in the available data of Lutjewad is that there are long periods of missing data from mid January to mid February and from mid December onward. In Cabauw some smaller gaps occur in the summer. Long periods of missing data are in November and December.

To make the differences between the simulated data and the observation better visible, the concentration of all tracers is summed to determine the total methane CH₄ concentration in Lutjewad and Cabauw. To sum these tracers, first the background concentration is subtracted from each tracer. Next the residue, the excess concentrations on top of the background, which is the contribution of the emission from a specific sector (e.g. agriculture, waste, energy etc.), is summed and finally the background is added again to end up with the total CH₄ concentration. The graphs of this total concentration of the tracers are shown in figure 8 for Lutjewad and Cabauw. Again the simulation output is plotted together with the observations.

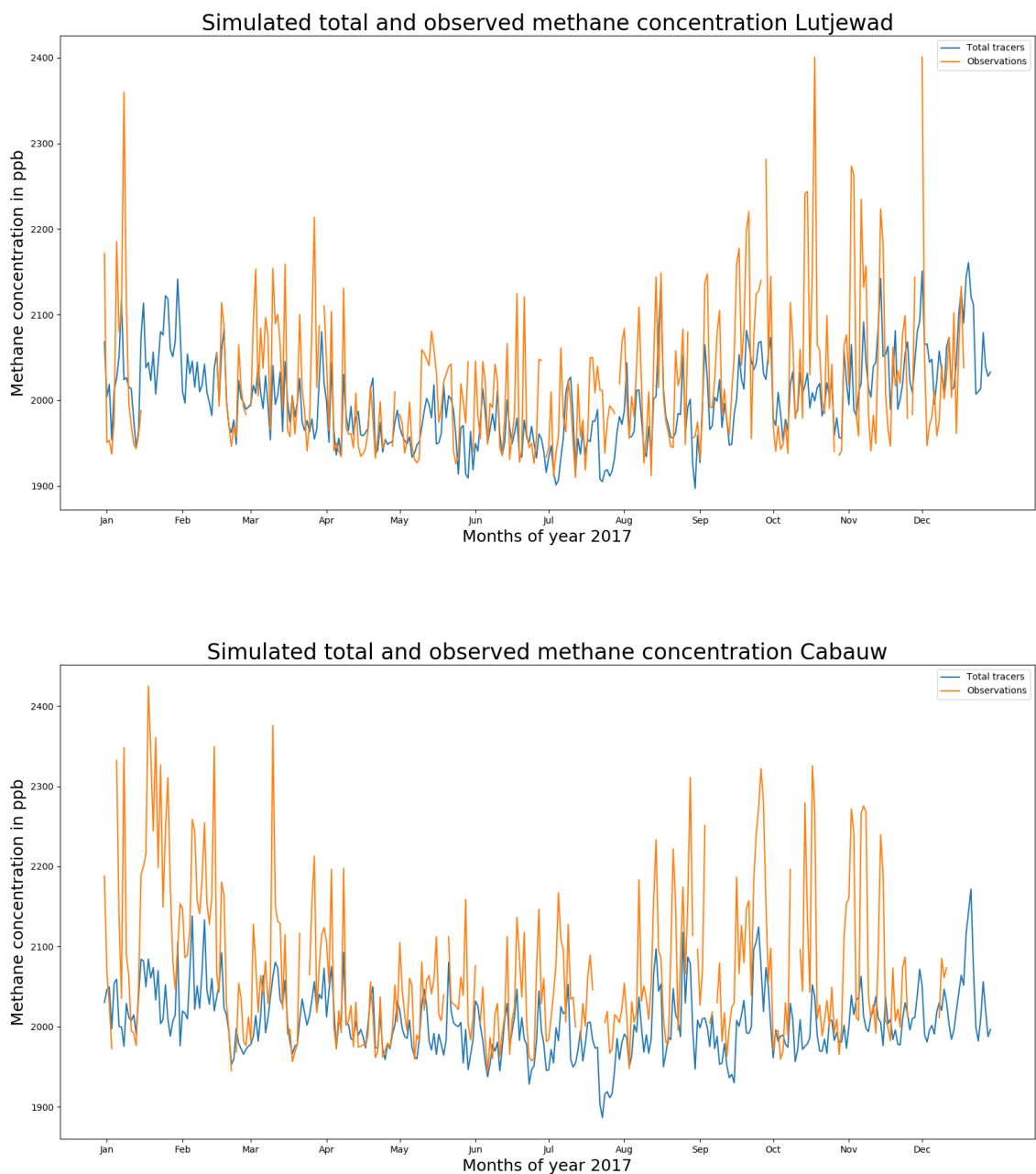


Figure 8: The methane concentration of the sum of all simulated tracers plus the background concentration (blue) and the observations (orange) are plotted for Lutjewad (top) and Cabauw (bottom) for 2017.

The total CH_4 concentration of all tracers is often slightly below the observed CH_4 concentrations, especially in Cabauw. High peaks in the observed methane concentration are often represented by peak concentration in the simulation, although these concentration peaks in the simulations are not as high as observed. A seasonal variability in concentration occurs in both the observation and the simulations, with

higher concentrations in autumn and winter. This variability is stronger in Lutjewad than in Cabauw.

The average excess concentration for each tracer, is shown in table 2. This is the CH₄ concentration contribution from the individual emission sectors. In this analysis the background used in the simulations is used to calculate the excess concentration both for the simulations and the observations. The average concentration of the sum of all tracers, together with the background, is also given, as well as the average observed concentration.

Table 2: Average CH₄ concentration in ppb for every tracer on top of the background, the total of the tracers and the observations in Lutjewad and Cabauw.

Source	Lutjewad	Cabauw
Agriculture	43.09	46.75
Other Ind.	0.10	0.15
Chem Ind.	0.06	0.13
Refineries	0.13	0.26
Energy	9.42	10.41
Transport	0.18	0.33
Consumers	1.38	2.22
Construction	0.00	0.00
Waste	12.92	14.26
Water pur.	0.04	0.11
Waste Water	1.90	2.23
Trade	0.05	0.13
Nature	4.07	4.80
Background	1926.31	1924.19
Total Tracers	1999.66	2005.99
Observations	2021.81	2072.40

On average, CH₄ emissions from agriculture add the highest concentration to the total CH₄ concentration. In Lutjewad this is about 43 ppb and in Cabauw 47 ppb in 2017. Waste and energy are the second and third highest contributors to the excess methane concentration induced by emission in the Netherlands. For all individual tracers, the excess CH₄ concentration is slightly larger at Cabauw than at Lutjewad. The total excess concentration induced by all sources is 74 ppb at Lutjewad and 82 ppb at Cabauw. The total CH₄ concentration induced by all sources is higher at Cabauw than at Lutjewad. However, the simulations still underestimate the observed concentration more at Cabauw than at Lutjewad. At Cabauw the observations are on average 66.5 ppb higher than the simulations. At Lutjewad this difference is only 22 ppb.

Next, the correlation of the tracers with the observations is determined to gain insight in the ability of the WRF-Chem simulations to reproduce the variability in methane concentration in 2017, i.e. the peak

event and seasonal variability as shown in figure 8. The correlations between the variability in simulated excess CH₄ concentration per tracer and observed excess CH₄ concentration is determined. Table 3 shows the correlation coefficients determined with the Pearson method. A coefficient of -1 means the datasets are exactly anti-correlates, 0 means there is no correlation and 1 means the datasets are fully correlated. These correlation coefficients are determined using day averaged CH₄ concentrations. For this reason, the diurnal variability is not covered in these correlation coefficients.

Table 3: Correlation coefficients of the trends in CH₄ concentration for every tracer compared to observations in Lutjewad and Cabauw. The darkness of the color green indicates the magnitude of the coefficient.

Source	Lutjewad	Cabauw
Agriculture	0.61	0.62
Other Ind.	0.64	0.33
Chem Ind.	0.48	0.17
Refineries	0.58	-0.04
Energy	0.48	0.65
Transport	0.62	0.43
Consumers	0.65	0.48
Construction	0.08	0.06
Waste	0.22	0.15
Water pur.	0.32	0.51
Waste Water	0.53	0.39
Trade	0.46	0.21
Nature	0.45	0.49
Background	0.08	0.08
Total Tracers	0.59	0.61

The correlation in trends between the individual tracers and the observation is approximately equal for agriculture in Lutjewad and Cabauw. Besides agriculture, in Lutjewad, other industry, refineries, transport and consumers have the highest correlation coefficients, around 0.6. Chemical industry, energy, waste water, trade and nature are also sources that are fairly well correlated with the observed methane concentration, with coefficients around 0.5. Especially the trends in the construction tracer correlate badly with the observations. However, the emissions and excess methane concentration of construction are also the lowest of all methane sources (see table 2). Therefore, the methane emissions from construction have a minor influence on the total CH₄ concentration in Lutjewad. In Cabauw the same holds for the construction source. Moreover, in Cabauw the refineries tracer is also poorly correlated with the observations, in contrast with

the correlation in Lutjewad. Furthermore, other industry, chemical industry, transport, consumers, waste water and trade have lower correlation in Cabauw than in Lutjewad. Energy, water purification and nature have higher correlation coefficients in Cabauw than in Lutjewad. The background shows in both locations a poor correlation with the observations. This is because peak events and trends are caused by local methane emissions in combination with meteorological conditions. During calm weather conditions (e.g. low wind speeds) emitted CH₄ is less transported and mixed in the atmospheric layer near the surface. This can lead to temporal local accumulation of CH₄ in the surrounding of large sources or areas of high emissions (Lu et al., 2019, Yuval et al., 2020). Another possible cause for temporal peak CH₄ concentrations at measurement locations, is the wind direction. When wind blows from a direction in which a large source or an area of high CH₄ emission is located, CH₄ concentrations detected at a measurement location might be above average (Saha et al., 2013). This influence of wind direction on the CH₄ concentration at the measurement locations is analyzed and discussed in section 3.3.

3.1.2 Methane concentration per month

The correlations of the simulation with observations, shown in the previous section, were only analyzed for the full year of 2017. To make the correlation in trends throughout 2017 more visible, the correlation coefficients are determined for every month. This way, differences per month in the correlation of the simulated variability with the observed variability, become clear. The correlation coefficients per tracer per month are shown in table 4 for Lutjewad and table 5 for Cabauw.

Table 4: Correlation coefficients of the trends in CH₄ concentration per month per tracer compared to observations in Lutjewad. Day averaged values are used for determining the correlation. The darkness of the color green indicates the magnitude of the positive correlations coefficients. The magnitude of the negative correlation coefficients are indicated by the darkness of the color red.

Month	Agri	Other Ind	Chem Ind	Ref	Ene	Trans	Cons	Constr	Waste	Water pur	Waste Water	Trade	Nature	Back-ground	Total Tracers
Jan	0.49	0.71	0.15	0.71	0.44	0.57	0.57	0.33	-0.09	0.30	0.33	0.31	0.41	-0.16	0.47
Feb	0.88	0.61	0.60	0.57	0.57	0.78	0.75	0.59	0.53	0.60	0.60	0.76	0.92	0.61	0.94
Mar	0.47	0.57	0.29	0.49	0.54	0.50	0.58	-0.27	0.11	0.09	0.54	0.14	0.15	-0.07	0.45
Apr	0.91	0.83	0.72	0.66	0.38	0.82	0.88	0.63	0.20	0.77	0.71	0.82	0.88	-0.07	0.81
May	0.74	0.65	0.68	0.64	0.09	0.62	0.69	-0.09	0.25	0.39	0.58	0.47	0.48	-0.30	0.55
Jun	0.66	0.55	0.68	0.55	0.36	0.60	0.62	0.21	-0.03	0.27	0.36	0.39	0.37	-0.20	0.57
Jul	0.55	0.57	0.57	0.55	0.33	0.53	0.60	0.11	0.23	0.42	0.49	0.45	0.34	-0.52	0.38
Aug	0.66	0.73	0.64	0.72	0.55	0.71	0.73	0.31	0.54	0.41	0.75	0.59	0.45	-0.13	0.67
Sep	0.56	0.56	0.60	0.57	0.40	0.58	0.60	0.04	0.46	0.17	0.62	0.24	0.19	0.33	0.71
Oct	0.68	0.72	0.85	0.50	0.70	0.69	0.72	0.19	0.15	0.12	0.54	0.40	0.48	-0.66	0.57
Nov	0.43	0.76	0.29	0.70	0.63	0.54	0.57	0.10	0.22	0.13	0.43	0.43	0.33	-0.52	0.33
Dec	0.64	0.20	-0.25	0.22	0.28	0.39	0.38	0.61	0.06	0.39	0.04	0.39	0.47	0.34	0.67

Strong differences occur in the magnitude of the correlation coefficients for different months. For agriculture for example, the lowest correlation with the observations is found in November, with a coefficient

of 0.43. While in April the correlation is 0.91. The background concentration shows a very poor correlation with the trends in the observations. In some months the trends in the background concentration even seems to be anti-correlated with the observation. Table 4 also shows that there are some months in which almost all tracers have a relatively good correlation with the observations, such as in February, April and August. The simulated concentrations in January, March and December show a relatively low correlation for most of the tracers. The correlation coefficients per tracer per month for Cabauw are shown in the table below.

Table 5: Correlation coefficients of the trends in CH₄ concentration per month per tracer compared to observations in Cabauw. Day averaged concentration values are used for determining the correlation. The darkness of the color green indicates the magnitude of the positive correlations coefficients. The magnitude of the negative correlation coefficients are indicated by the darkness of the color red.

Month	Agri	Other Ind	Chem Ind	Ref	Ene	Trans	Cons	Constr	Waste	Water pur	Waste Water	Trade	Nature	Back-ground	Total Tracers
Jan	0.44	0.26	0.01	0.05	0.29	0.25	0.24	0.01	-0.31	0.61	0.01	0.05	0.30	-0.23	0.30
Feb	0.63	0.07	-0.13	-0.19	0.52	0.40	0.45	0.05	0.26	0.35	0.24	0.22	0.42	0.39	0.66
Mar	0.72	0.14	-0.16	-0.35	0.70	0.55	0.55	0.42	0.24	0.58	0.45	0.39	0.70	-0.15	0.68
Apr	0.90	0.65	0.58	0.35	0.62	0.74	0.81	0.59	0.43	0.67	0.64	0.62	0.77	-0.13	0.87
May	0.46	0.18	0.21	-0.13	0.22	0.47	0.46	0.17	0.19	0.54	0.34	0.35	0.55	-0.11	0.38
Jun	0.80	0.06	0.39	-0.29	0.67	0.76	0.74	0.60	0.28	0.47	0.65	0.65	0.75	-0.14	0.79
Jul	0.80	0.42	0.31	0.12	0.62	0.60	0.63	0.01	0.29	0.27	0.48	0.58	0.70	-0.54	0.66
Aug	0.80	0.44	0.29	-0.09	0.77	0.81	0.80	0.71	0.51	0.56	0.61	0.75	0.79	-0.27	0.81
Sep	0.73	0.30	0.11	-0.33	0.85	0.58	0.62	0.04	0.10	0.33	0.39	0.35	0.60	0.29	0.71
Oct	0.85	0.49	0.20	-0.05	0.83	0.66	0.68	-0.33	0.10	0.62	0.29	0.44	0.78	-0.59	0.65
Nov	0.31	0.46	0.04	0.15	0.58	0.10	0.11	0.11	0.05	0.55	0.27	-0.17	0.14	-0.59	0.08
Dec	0.62	-0.87	-0.91	-0.95	0.32	0.08	0.01	-0.59	-0.97	0.64	-0.91	0.09	0.55	-0.42	-0.18

The correlation coefficients of the simulation of methane concentration at Cabauw do also differ strongly per month. Again, the background concentration has a poor correlation with the observations. For Cabauw the refineries tracer shows a bad correlation for almost every month as well. In April and August most tracers had a relatively good correlation with the observations at Cabauw, as was also the case at Lutjewad. In February the correlation for most tracers is not above average at Cabauw. In January most tracers had relatively bad correlation at Cabauw. The same holds in May and November. In December there is even very strong anti correlation for some tracers. However, it has to be taken into account that the observational data of December at Cabauw is very sparse. There is only measurement data for two days in December. This means the correlation coefficients are based on a very short period in time, making it not representative for the variability in the whole of December.

As described above, table 4 and 5 show that the tracer for the agricultural methane emission overall has the best correlation with the observations at both Lutjewad and Cabauw. The background has very low correlation in almost all months for both locations. This is the same for the construction sector. From this can be concluded that the variability in the CH₄ concentration on timescales of days and weeks is mainly driven by (local) emissions within the simulation domain. In April and to a lesser extent in August, a relatively high correlation for almost all tracers at both Cabauw and Lutjewad is found. On the other hand

in January, November and December, a relatively low correlation for almost all tracers at Lutjewad and Cabauw is found. This suggests that the correlation of the variability in the simulation to the variability in the observations, is not merely determined by local emission events. Correlation is high, or low, for the same months at Lutjewad and Cabauw. This can be caused by influences that play a role on at least a spatial scale of several hundreds of kilometers, most likely meteorological conditions.

3.2 Diurnal cycle

3.2.1 Methane concentration

In the previous section only diurnal averaged concentration data was used for analysing the correlations. In this section the hourly data is used to analyze the occurrence of a diurnal cycle in the CH₄ concentration. Diurnal variability is expected because of the fluctuation in the boundary layer height between day and night time, discussed in the next subsection. Another reason is the variability in emissions from some methane sources over the day. This variability in emissions was not implemented in the first simulation run (see section 1). An estimation of this variability for several emission sources was implemented in the second run. This is implemented for the tracers other industry, chemical industry, energy, transport and consumers. The average diurnal range in methane concentration per month, for both runs and the observations, is shown in figure 9 for Lutjewad and 10 for Cabauw.

Diurnal cycle of sum of tracers and observations in Lutjewad

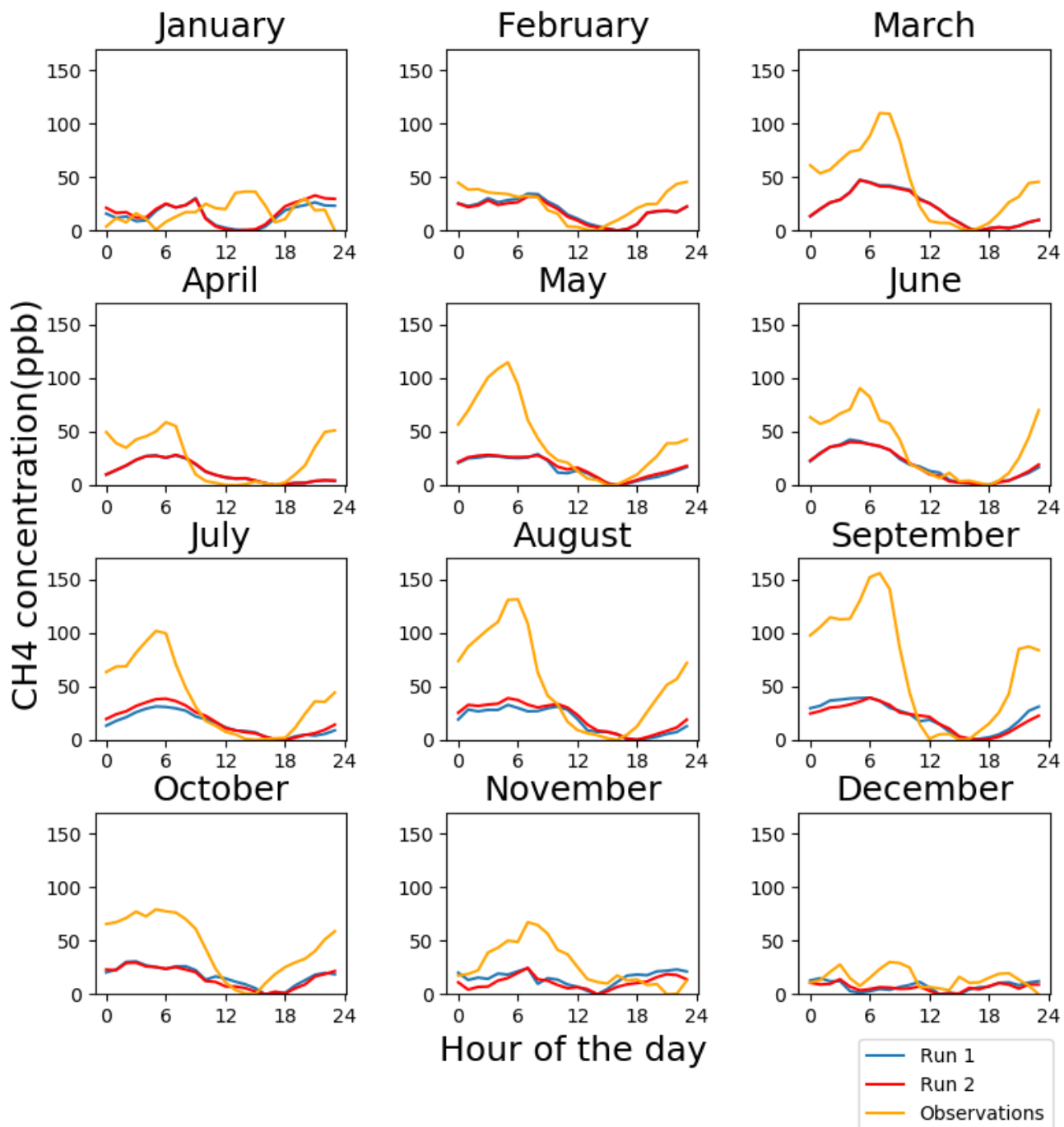


Figure 9: Average diurnal range of methane concentration per month in 2017 at Lutjewad. The plots show the total of tracers for the first run without diurnal emissions profile (blue), the second run with diurnal emissions profile (red) and observations in Lutjewad(orange).

The observations in Lutjewad show no clear diurnal cycle for January and February(see figure 9). From March onward, a diurnal cycle is observed with increasing amplitude until September and slightly decreasing thereafter. The strongest diurnal cycle occurs in September with CH₄ concentrations being on average 150 ppb higher in the early morning than in the afternoon. The first run, without diurnal variability in the emissions, shows a weaker diurnal cycle in the CH₄ concentration. February and December do not have a distinct diurnal cycle. The amplitude of the diurnal cycle fluctuated over the year, being smaller during autumn and winter. March has the largest amplitude with CH₄ concentration being 50 ppb higher in the early morning than in the late afternoon. Overall, the amplitude of the simulated diurnal cycle in the methane concentration in Lutjewad, is underestimated. This underestimation is largest in spring and summer. The diurnal cycles found in the second run, differ only slightly from the diurnal cycles found in the first run. In the months July and August, the simulated diurnal cycle came a little closer to the observed diurnal cycle, than in the first run. However, for September and November, the diurnal cycle of the second run represents the observations a little less well. Overall, adding diurnal variability in some of the emission sources, does not substantially change the diurnal cycle in the simulated methane concentration at Lutjewad.

The average diurnal range per month for Cabauw is shown in figure 10, on the next page.

Diurnal cycle of tracers and observations in Cabauw

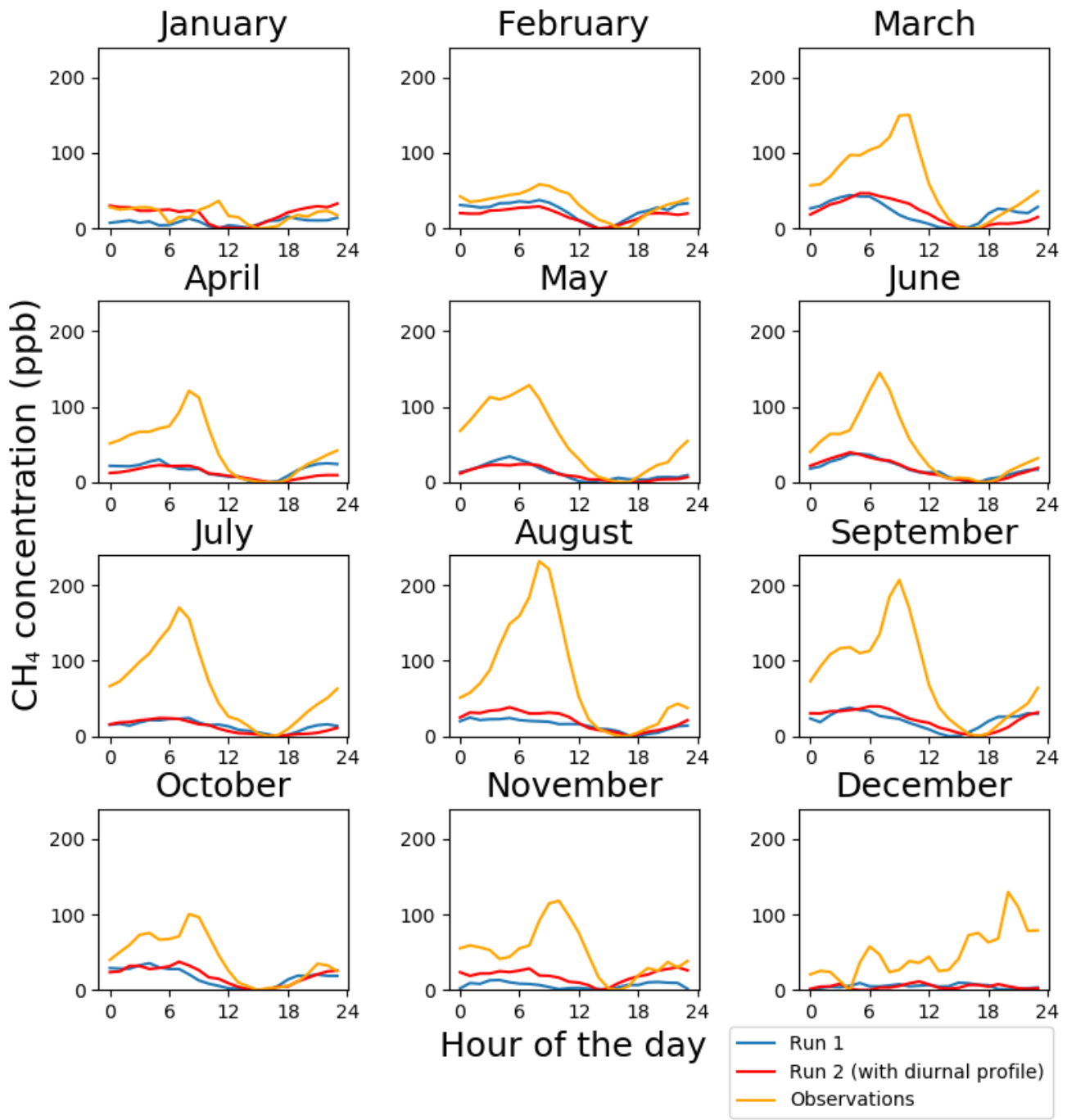


Figure 10: Average diurnal range of methane concentration per month in 2017 at Cabauw. The plots show the total of tracers for the first run without diurnal emission profile (blue), the second run with diurnal emissions profile (red) and observations in Cabauw (orange).

The observations in Cabauw show the same increasing amplitude of the diurnal cycle each month until September. After September the amplitude stays approximately the same. The maximum amplitude occurs in August. In that month the observed methane concentrations in Cabauw are on average 225 ppb higher in the early morning than in the late afternoon. The simulated methane concentration in Cabauw has a smaller diurnal range than that is observed. In January, November and December no clear diurnal cycle occurs. The strongest diurnal cycle occurs in March, June and September, the same as for Lutjewad. The average diurnal fluctuation is highest in March and is 45 ppb. Apart from January and February, the simulations underestimate the diurnal range in the methane concentration at Cabauw. The second run shows only slightly different diurnal cycles than the first run. A small improvement of agreement of the simulated diurnal cycle with the observed diurnal cycle occurs in almost every month, except February and April. Although the effect of the diurnal variability in the emission on the diurnal cycle in the methane concentration is larger in Cabauw than in Lutjewad, it still explains only a minor part of the discrepancy between the simulation and the observation. There must be another cause of the difference between simulations and observations in the diurnal range of the methane concentration.

3.2.2 Boundary layer height

Another cause of the occurrence of a diurnal cycle in the methane concentrations in Lutjewad and Cabauw, is the diurnal variability in the boundary layer height (BLH) in the atmosphere. As explained in section 2.5, the height of the boundary layer fluctuates over the day. The height, or thickness of this layer influences the concentration of the gasses in this layer. If there is a poor representation of the diurnal variability of the boundary layer height by the WRF-Chem simulation, this can be an explanation for the weaker diurnal cycle in the methane concentration found in the simulation. The simulated boundary layer height is compared with measurements of the boundary layer height at Cabauw. The data is presented again as the monthly average 24-hour variability. This is shown in figure 11. The BLH in the measurements is determined by the vertical gradient in particle concentration. The BLH in the simulations is determined using meteorological parameters (see section 2.5). The measurements of the boundary layer height at Lutjewad did not produce reliable data for most of the months of 2017. Therefore, only the boundary layer height at Cabauw is considered in this analysis.

Diurnal cycle in boundary layer height per month

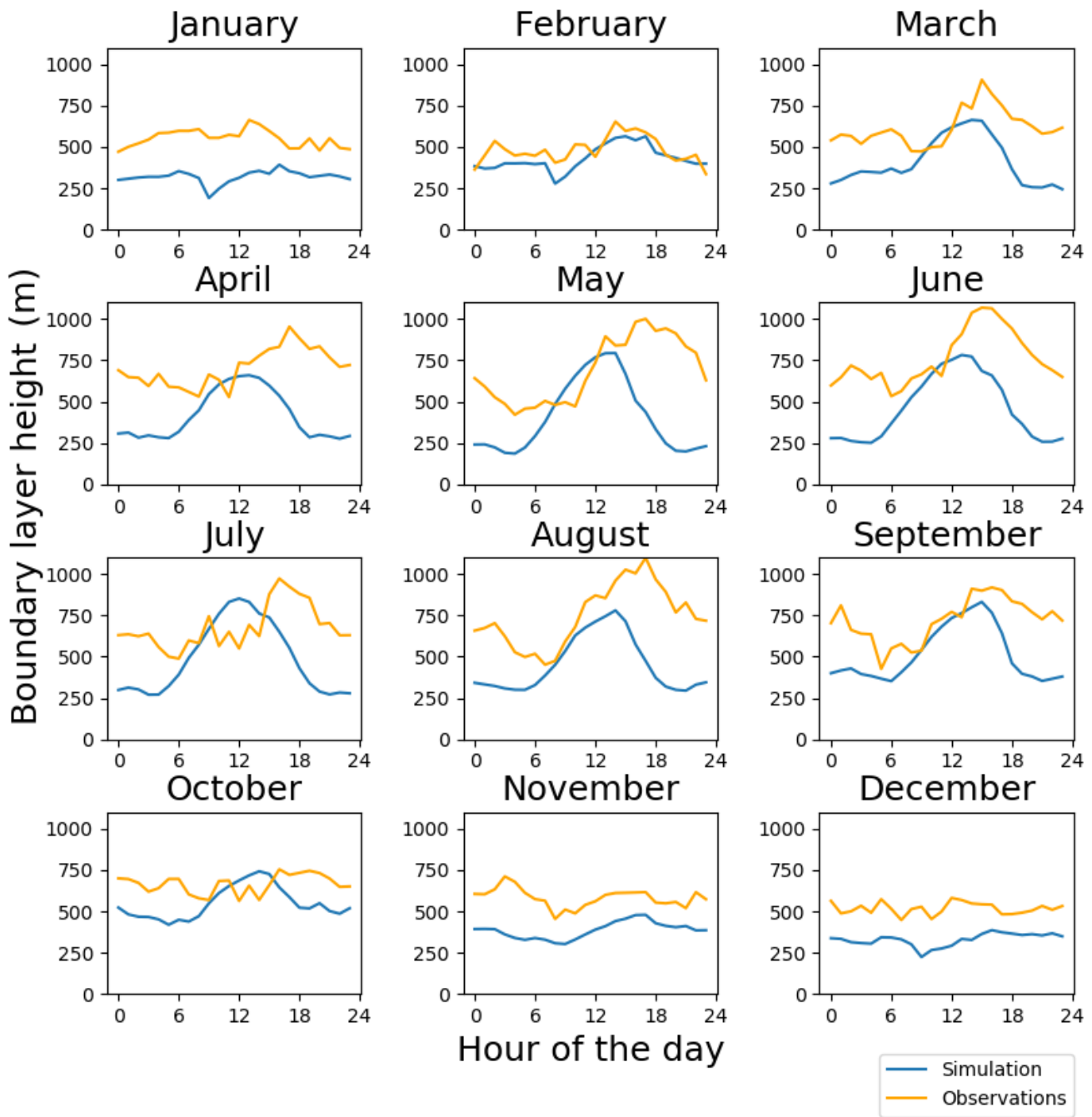


Figure 11: Average diurnal cycle of the boundary layer height per month in 2017. The plots are for the simulation (blue) and observations in Cabauw (orange).

The simulations represent the overall shape over the diurnal cycle in the boundary layer height in Cabauw fairly well for most months. The height of the boundary layer is on average lower in the simulations than the observed height. For most months this difference is 200-250 meters. Furthermore, the diurnal cycle in the simulation has a phase shift with respect to the observed diurnal cycle. The troughs and peaks in the boundary layer height occur several hours earlier in the simulation than in the observations. This might be caused by the different definitions used for determining the BLH in the simulations and the measurements. Despite of these differences, the range between minimum and maximum boundary layer height for every month are about equal for the simulation and observations. The ratio between nighttime BLH and daytime BLH is even larger in the simulations than in the observations. The simulated daytime BLH is about 4 times the nighttime BLH during the summer months. In the observations this daytime nighttime ratio of the BLH is approximately 2 in summer. Based on the difference in ratios between the simulation and the observations it could be expected that the diurnal variability in the simulated CH₄ concentration would larger than in the observed CH₄ concentration. However, the opposite is found in this analysis (see section 3.2.1).

3.3 Influence of wind direction on tracers concentration

3.3.1 Simulated wind direction compared with observations

As explained in the introduction section of this thesis, the wind direction is expected to influence the magnitude of the excess methane concentration induced by CH₄ emission from a specific source (tracer) on top of the background. Different methane sources are located around the measurement locations. When the wind blows from a certain wind direction, emitted methane from a nearby source can be blow toward the measurement site and will influence the total CH₄ concentration there. While with an opposite wind direction, the emission from a nearby source will be blown away from the measurement site and this source will not affect the CH₄ concentration at this site. The observed wind direction from the ERA-Interim data is used as input for the boundary conditions in the WRF-Chem simulations. The results discussed in this section focus on this influence of the wind direction. First of all, the simulated wind direction in Lutjewad and Cabauw are compared with the observations. Figure 12 shows the 24 hour average wind direction in 2017 in Lutjewad. Note that the observed wind direction in Lauwersoog is used instead of that in Lutjewad, because of a lack of availability of wind data in Lutjewad. Lauwersoog is located 10 km to the west of Lutjewad.

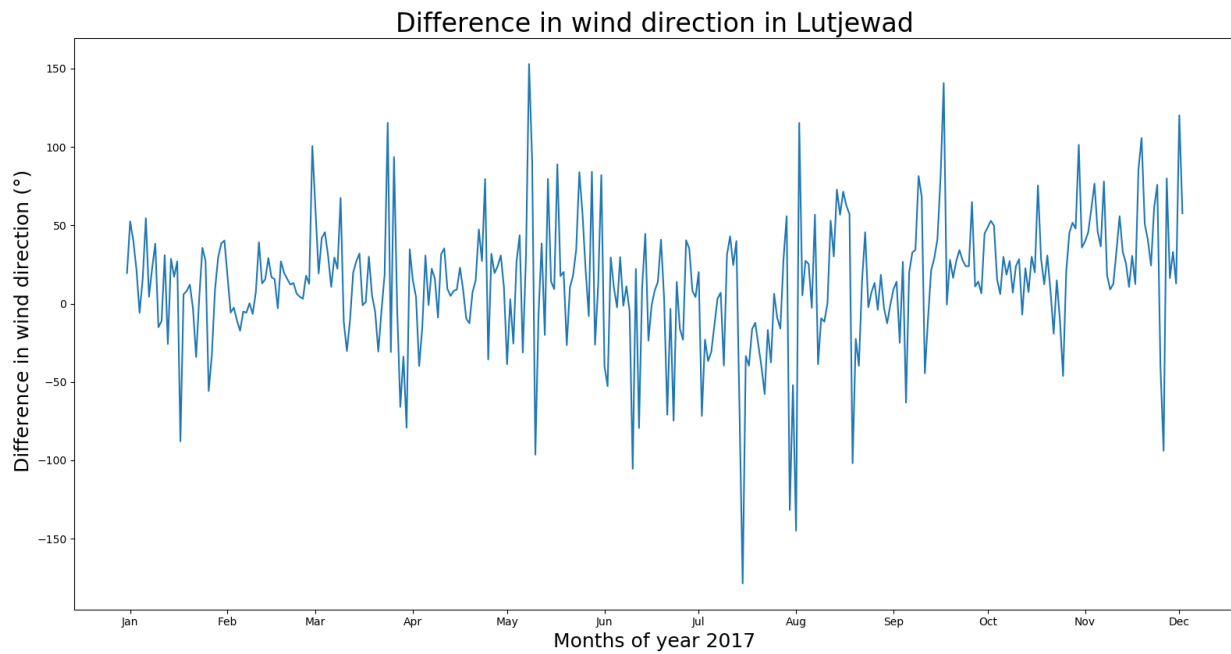
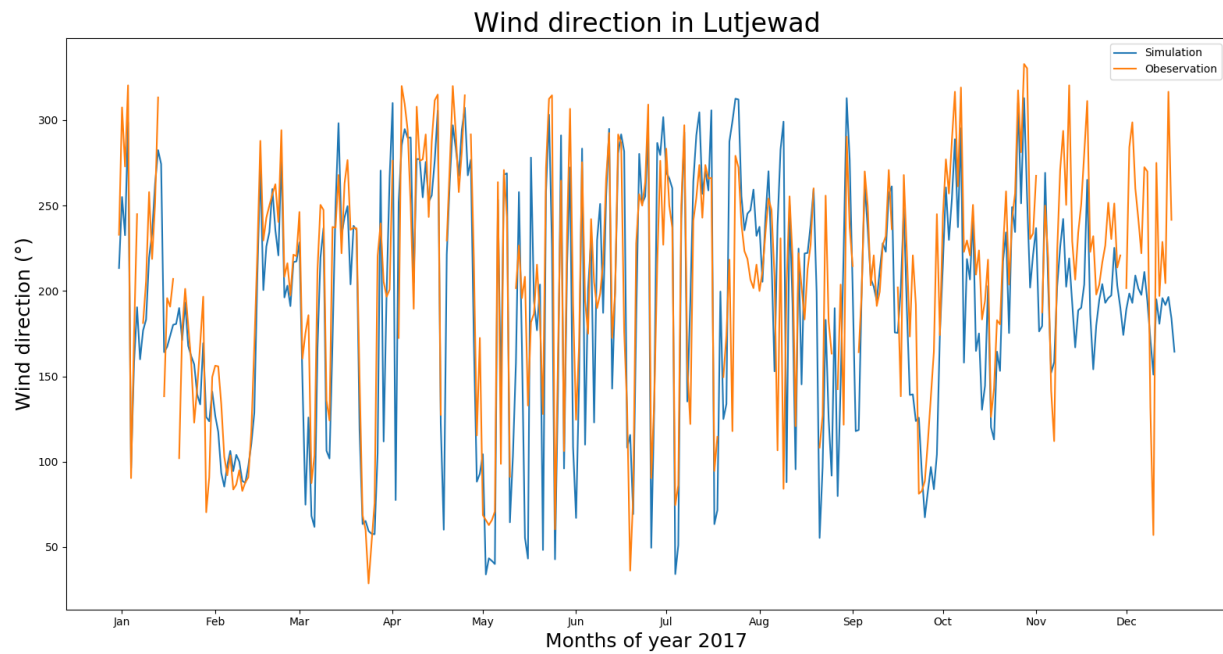


Figure 12: The simulated wind direction(blue) in Lutjewad and the observed wind direction (orange) in Lauwersoog for the year 2017, are shown in the top graph. The differences in wind direction between the observation (in Lauwersoog) and the simulation(in Lutjewad) are shown in the bottom graph.

From the top graph in figure 12 it becomes clear that both observation and simulation show rapid changes in wind direction, especially in spring and summer time. Most peaks in the observation seem to coincide with peaks in the simulated wind direction. The lower graph shows the difference in degrees between observations and simulations. Although most of the year the differences are between -50 and +50 degrees, there are several peaks in which the difference is more than 100 degrees. This sometimes large difference in observed and simulated wind direction, can be caused by the very rapid changes or narrow peaks not being fully represented in the simulations. The meteorological input data is only update every 6 hours. This means that the observed wind direction can deviate from the simulated wind direction over the time period of 6 hours. The absolute mean difference between observations and simulations is 42 degrees. The average real difference is 13.2 degrees between observations and simulations. On average the observed wind direction is turned 13.2 degrees clockwise with respect to the simulated wind direction. This might be caused by Lutjewad (simulation) and Lauwersoog (observations) being located 10 km apart.

The simulated and observed wind direction in 2017 in Cabauw are shown in figure 13.

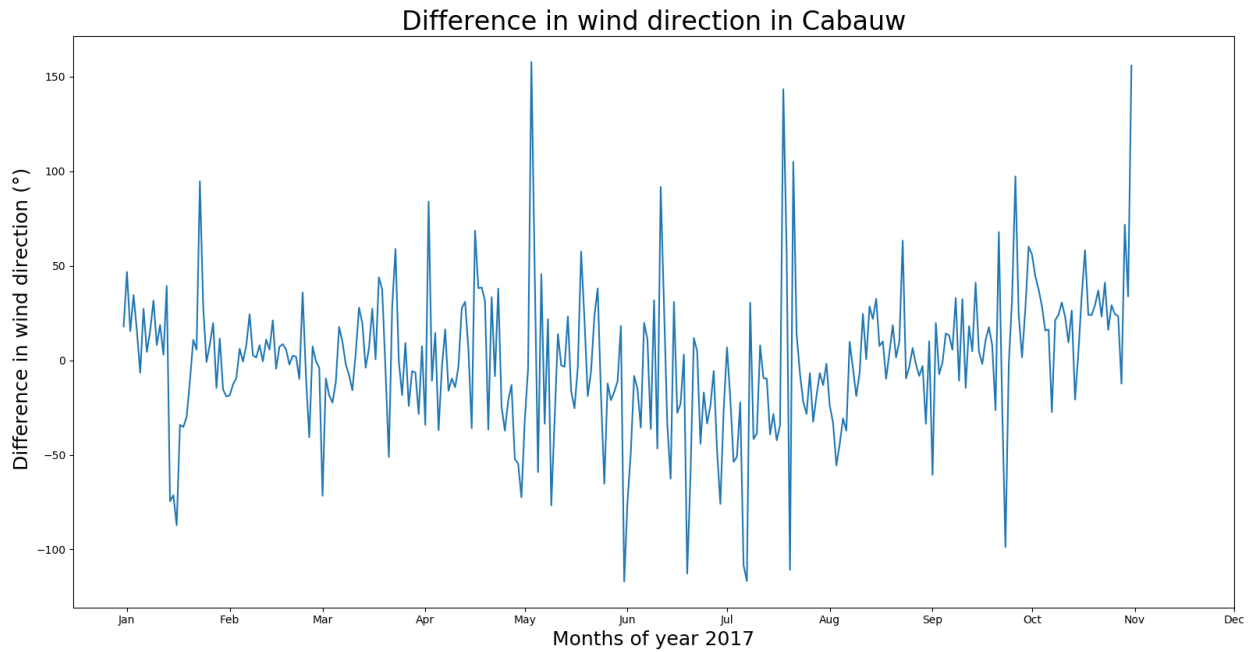
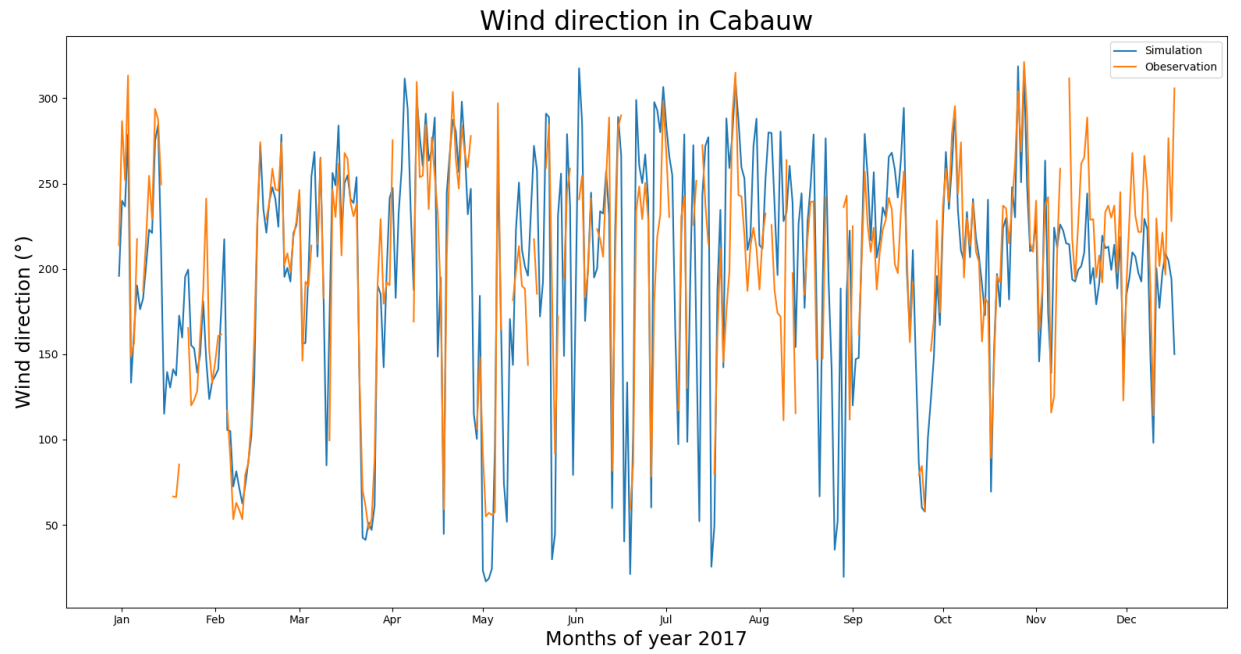


Figure 13: The simulated wind direction (blue) and the observed wind direction (orange) in Cabauw in 2017, are shown in the top graph. The difference in wind direction between the observation and the simulation is shown in the bottom graph.

The wind direction in Cabauw shows the same features as in Lutfjewad. Rapid changes throughout the year occur due to the influence of changing atmospheric pressure systems (van Doorn et al., 2000). The difference between the simulated and observed wind direction fluctuates mainly between -50 and +50 degrees in 2017. Several large peaks of more than 100 degrees difference occur mainly in summer when changes in wind direction are the strongest. The absolute mean difference between observation and simulation is 40 degrees. The average real difference is -0.3 degrees between observation and simulations in Cabauw. This means that the observed wind direction is turned only 0.3 degrees counterclockwise with respect to the simulations, on average.

3.3.2 Methane concentration depending on wind direction

The effect of the wind direction on the excess methane concentration of every tracer is analyzed by making wind roses for every tracer. The wind roses are made using the hourly excess methane concentration of every tracer. This concentration is normalized according to the average excess CH₄ concentrations given in table 2. This normalized excess CH₄ concentration is categorized in 8 different wind directions of 45 degrees. For the hourly concentration data, the methane concentration of every tracer is categorized according to the direction the wind was blowing that hour. Only the data points for which the simulated and the observed wind were blowing from the same direction, are used in this analysis. Therefore, only 2726 data points at Lutfjewad and 2610 data points at Cabauw of the in total 8761 data points per location are used. Clearly the wind did not blow from every direction the same amount of time. For Lutfjewad the wind blew the least amount of time from the north-northeast, having only 112 data points (4% of the used data points) in whole 2017. The wind direction occurring most often was south-southwest, with 902 data points (33% of used data points). In Cabauw the least occurring direction is south-southeast with 104 data points (4% of used data points). The most frequent wind direction for this location is south-southwest, having 969 data points (37% of used data points). The wind roses for Lutfjewad are shown in figure 14 and for Cabauw in figure 15.

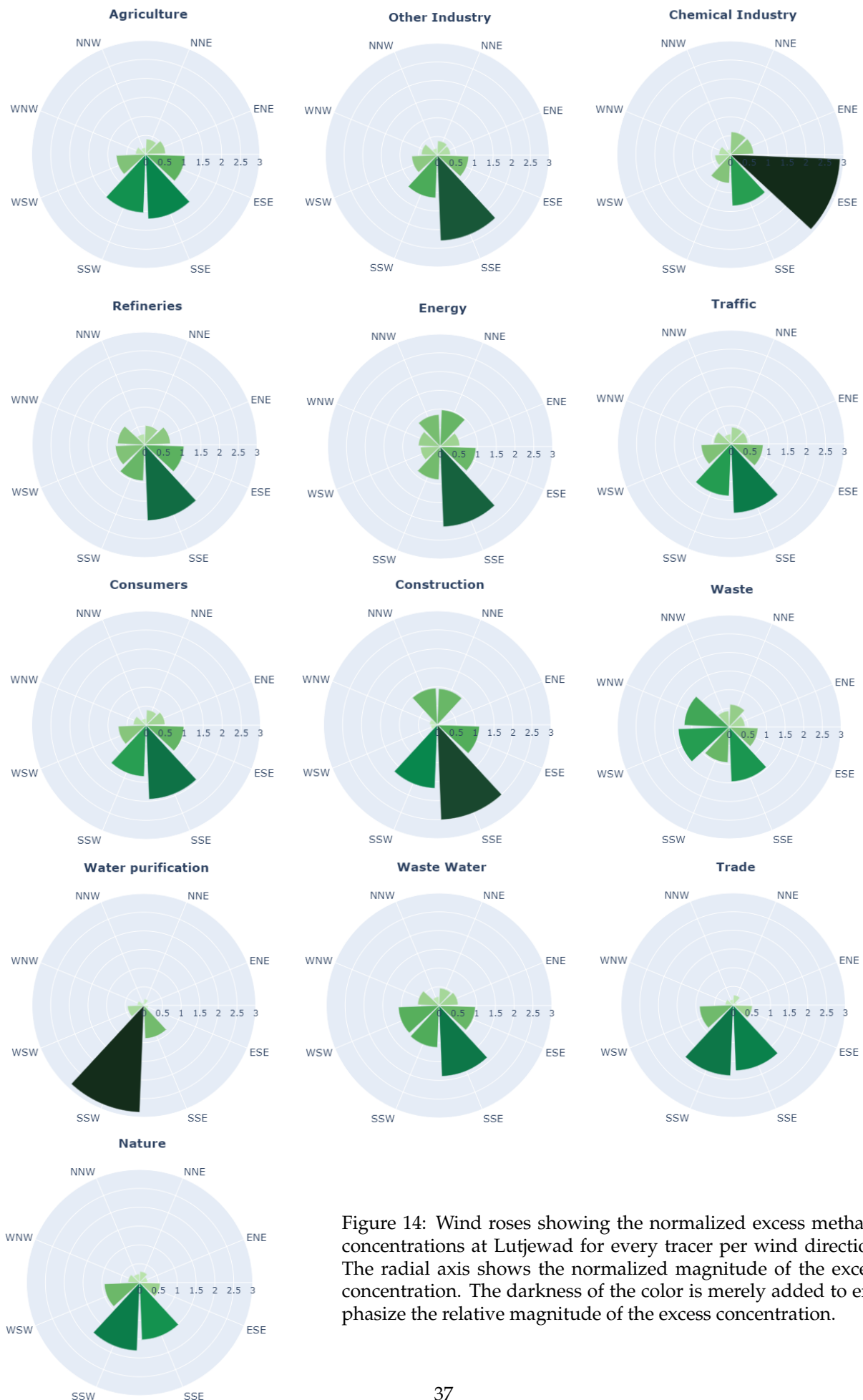


Figure 14: Wind roses showing the normalized excess methane concentrations at Lutjewad for every tracer per wind direction. The radial axis shows the normalized magnitude of the excess concentration. The darkness of the color is merely added to emphasize the relative magnitude of the excess concentration.

The tracer representing agricultural emissions shows an enhancement of 1.7 times the average excess CH_4 concentration by agricultural emission, when the wind blew from south-southeast direction. The excess concentration by the sectors chemical industry and water purification is even 2 times higher than the average excess concentration of these tracers, when the wind blows from east-southeast and south-southwest direction respectively. This might be caused by individual local sources. Concentrations from waste and energy, the second and third largest sources in Lutjewad, were about double the average excess concentration when the wind blew from the south-southeast. In the south-southeast direction of Lutjewad, the city of Groningen is located. This is the largest city within 100 kilometers from Lutjewad. From all wind roses it becomes clear that excess CH_4 concentrations induced by a tracers on top of the background, were on average higher when the wind blew from a southern direction. This can be explained by the fact that almost all local methane emission sources are located south of Lutjewad, while in the north the Waddensea stretches out.

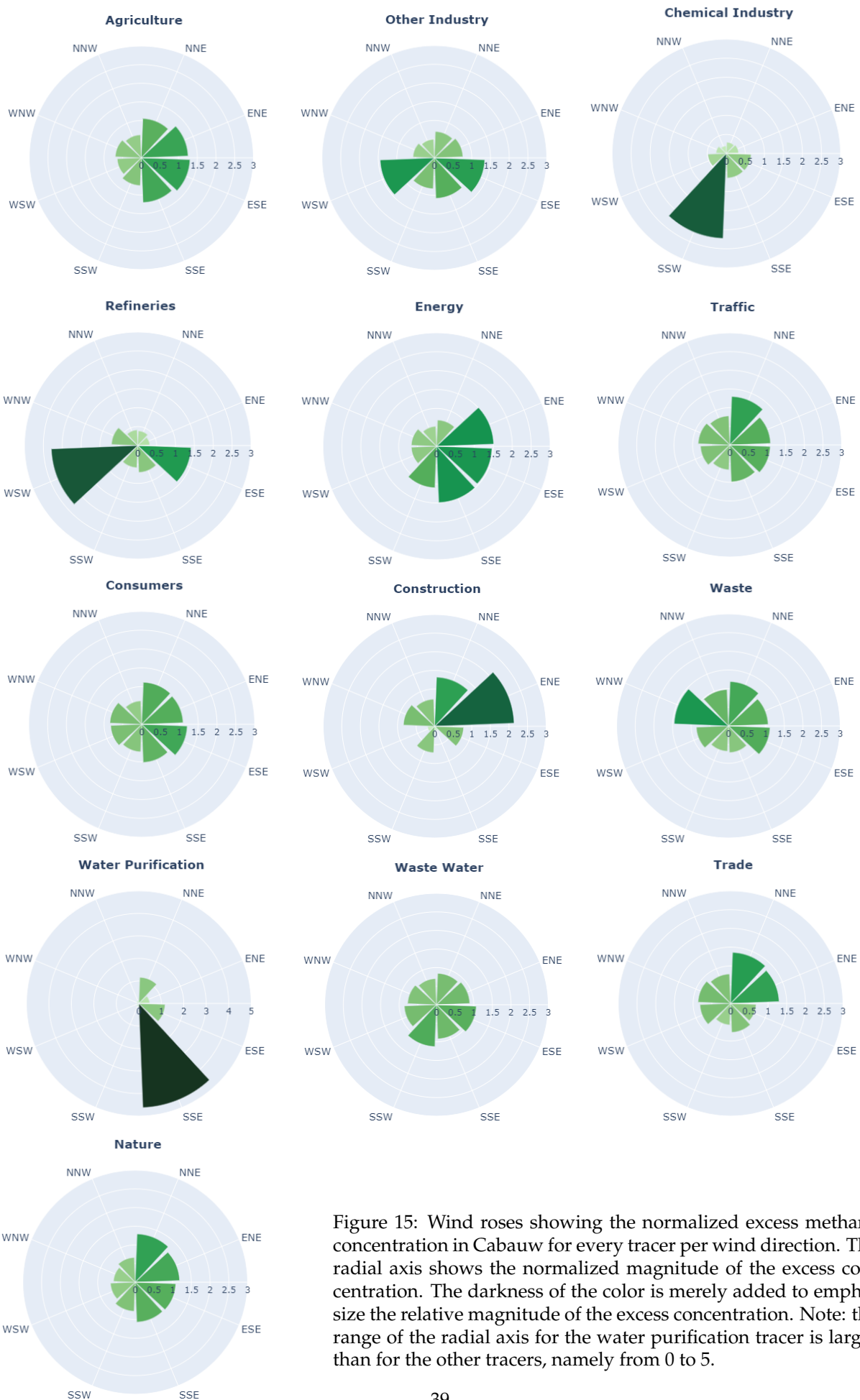


Figure 15: Wind roses showing the normalized excess methane concentration in Cabauw for every tracer per wind direction. The radial axis shows the normalized magnitude of the excess concentration. The darkness of the color is merely added to emphasize the relative magnitude of the excess concentration. Note: the range of the radial axis for the water purification tracer is larger than for the other tracers, namely from 0 to 5.

The tracer representing agricultural emissions at Cabauw shows an enhanced excess methane concentration up to 1.3 times the average excess concentration of this tracer, for eastern wind direction. This can be caused by the high agricultural emissions in eastern Brabant and eastern Utrecht with intensive livestock farming. For the energy source the enhancements occur for the same wind directions as for agriculture. Waste sources show the highest excess concentration of 1.5 times the average concentration, for wind blowing from the west-northwest. Excess concentration from refineries methane emission are largest for west-southwest wind. In this direction the harbor of Rotterdam is located with several large refineries. The largest excess CH₄ concentration for water purification occurs when the wind direction is from south-southeastern direction. The excess concentration from water purification is in this case almost 5 times as high as the average excess concentration.

To make a proper comparison of the dependence of the total simulated and observed excess methane concentration on the wind direction, the total excess CH₄ concentration of all tracers is compared with the total observed excess CH₄ concentration. The wind roses for the total of tracers and the observations are shown in figure 16.

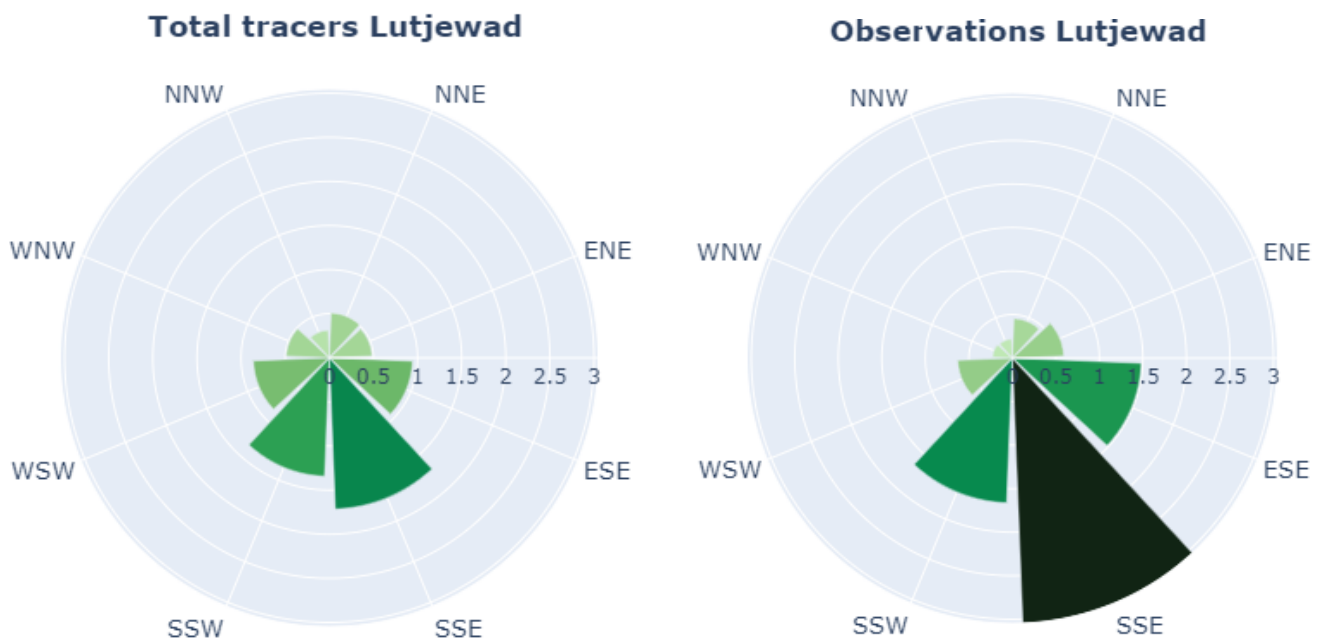


Figure 16: Wind roses are shown for the simulated total of tracers (left) and observations (right) in Lutjewad. The radial axis shows the normalized magnitude of the excess concentration. The darkness of the color is added to emphasize the relative magnitude of the excess concentration.

The simulation and observations both show the largest enhancement of excess methane concentration on top of the background, for south-southeastern wind. However, the excess concentration of the simulation in this wind direction is only 1.7 times the average concentration. For the observations the methane concentration on top of the background, with wind from the south-southeast direction, is more than 3 times the average concentration. This means that in reality the magnitude of the excess methane concentration is

more dependent on the wind direction than the simulation shows.

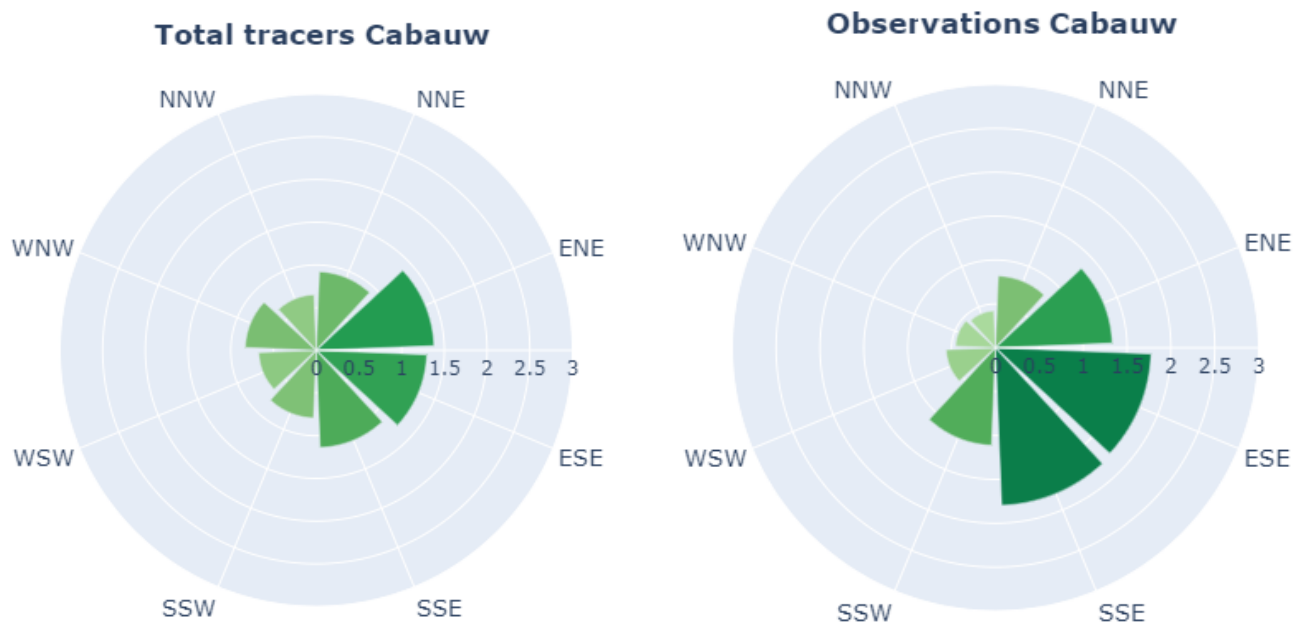


Figure 17: Wind roses for the simulated total of tracers (left) and observations (right) in Cabauw. The radial axis shows the normalized magnitude of the excess concentration. The darkness of the color is added to emphasize the relative magnitude of the excess concentration.

In the simulation the highest relative excess concentration in Cabauw occurs for wind from the east-northeast. The excess concentration for this wind direction is 1.4 times the average concentration. The observations in Cabauw show on average the highest excess concentration for wind from the east-southeast and the south-southeast. The concentration for wind from these directions is 1.8 times the average excess concentration. Thus, the wind direction for which the average excess methane concentration is highest is turned 45-90 degrees counterclockwise in the simulation, with respect to the observations. This might point to underestimated CH_4 emissions at the southeast of Cabauw. For example, agricultural emissions from Brabant might be higher in reality than estimated in the RIVM inventory. Furthermore, as also seen in Lutjewad, the simulation underestimates the dependence of the magnitude of the excess methane concentration on the wind direction.

3.4 Qualitative error analysis

All data used in this research is subject to uncertainties. Taking into account these uncertainties is necessary for a proper interpretation of the research data. Some information about the uncertainties for several of the input data used for the simulations is available. For the RIVM CH_4 emission inventory data only the standard deviation for national emissions is known. This standard deviation is 4.5% (RIVM, Emissieregistratie, 2020). On regional scale the uncertainties of emissions are probably higher. Uncertainties for point

sources are often unknown because they depend on reported emission from individual companies or other sources. For the EDGAR emission inventory no information about the standard deviation is provided. For the ERA-Interim meteorologic data used in this study, no information on the uncertainty is provided either. The average standard deviation of a single measurement of the CH₄ concentration in Lutjewad is 0.6%. For the measurements in Cabauw, no information about the standard deviation is provided. For the wind direction and boundary layer height data used in this research, no information about the uncertainties was provided.

The output data of the WRF-Chem simulations is a product of input data sets as mentioned above. The WRF-Chem model also uses several data sets included in the model, such as terrestrial data and boundary conditions for gases. The use of many different datasets of which some have no information about the uncertainties, together with the complex process involved in the WRF-Chem model, makes it hard to conduct a quantitative error analysis on the simulation output. For this reason and the limited time available, no quantitative error analysis is conducted in this study.

4 Discussion

This section presents a discussion on the interpretation of the results of this study. Furthermore, the research questions stated at the beginning of this thesis, are answered throughout this section. The final part of this section includes a discussion of the limitations of the data and research method used in this study. Recommendations for further research will be given.

4.1 WRF-Chem simulation and *in situ* observations compared

4.1.1 Seasonal variability

A seasonal cycle is found in the simulated and observed methane concentrations (see figure 7). CH₄ concentrations were lower during summer and higher during winter. This seasonality is probably caused by the higher removal rate of CH₄ with the OH radical during summer (Khalil and Rasmussen, 1983). This removal reaction of CH₄ with OH depends on the available shortwave solar radiation. Solar radiation is stronger on the northern hemisphere during summer than during winter. Although this chemical removal is not included in the simulation of CH₄, the boundary conditions do include this chemical removal. For this reason the background concentration is affected by the chemical removal. This results in the occurrence of a seasonal cycle in the concentration of every tracer.

4.1.2 Peak events

The peak events in the methane concentration in 2017 are largely represented by the simulated total methane concentration, see figure (8). The magnitude of the peaks in the simulated total methane concentrations is

lower than in the observations. The following four causes for this underestimation are addressed and discussed further below:

- Peak emissions of local sources during short periods of several days or weeks are not captured by the simulations.
- The simulated weather conditions deviate from the real weather conditions.
- Plume emissions are less concentrated in the simulations than in reality.
- Some large sources are underestimated.

These peak events in the observations might be caused by enhanced emissions of local sources during short periods of several days or weeks. Such enhancements or anomalies in CH₄ emissions from local sources are not represented by the WRF-Chem model, because it is difficult to take this into account in the emission used as input for the WRF-Chem model. Methane emissions from all sources are assumed to be constant for every hour in 2017. However, if such anomalies would be the cause, the simulation would not be expected to show coincident peaks with the observations. Instead, most peak events that occurred in the observed concentration are shown in the simulation, but the peaks are lower.

Another reason might be that the weather conditions simulated with the ERA-Interim data deviate from real weather conditions. Especially with calm weather with low wind speeds, methane can accumulate in the atmosphere near the sources. If these conditions are not well represented in the ERA-Interim data, the accumulation of methane in the simulation might be lower than in reality. This would result in lower peak concentrations. However, this is unlikely to be a large effect. With the use of nudging in the WRF-Chem model simulation, the weather conditions were forced to stay very close to the real weather conditions.

The most likely cause is that CH₄ emissions are averaged over the volume of the 3 km x 3 km grids in order to use it as input for the model. This means dense plume emissions from point sources are spread out over the volume of a grid in the simulation. In reality the concentration measured in such a plume can for this reason be denser than in the simulation, where the plume is spread out over a much larger area. During periods of regional accumulation of methane, local concentrations can become much higher in reality for short periods of time, because the emissions are more concentrated than in the simulations.

Another cause for this underestimation of the peak events could be the underestimation of the strengths of the local methane emission sources. If the local sources in a period emit less methane in the simulations than in reality, the accumulation of methane during calm weather conditions, will be less than it is in reality. In this case peaks in the methane concentration will be lower in the simulations. Peak events can also occur when wind is blowing from a direction where high CH₄ emissions occur. If in a specific direction from the measurement site larger amounts of methane are emitted than in other directions, the CH₄ concentration will peak at the measurement site when wind blows from this direction of higher CH₄ emissions. When emissions sources in this specific direction are underestimated the magnitude of the

peak CH₄ concentration will be underestimated. This underestimation of methane emissions would also explain the overall underestimated methane concentration in the simulation. Especially in Cabauw this underestimation of CH₄ concentration by the simulations is relatively large with 66.5 ppb on average.

4.1.3 Correlation per year

The correlation coefficients given in table 3 quantify the correlation between the variability in excess methane concentration in the simulation and the observations. In Lutjewad most tracers show correlation coefficients around 0.5 or higher. The variability in excess CH₄ concentration of the sectors construction, water purification and waste have a poor correlation with the observations. Construction and water purification are very small methane sources, which is the reason that they only have a minor influence on variability in the total methane concentration. The waste sector is the second largest methane source in both Lutjewad and Cabauw, but at both locations the correlation of the variability in excess CH₄ concentration of this tracer to the observations is poor. This might indicate that the waste emissions are underestimated in the simulations.

Another reason for the low correlation of the waste sector with the observations might be the spatial distribution of the waste CH₄ sources. As explained in section 3.1.1 peak events can occur when wind blows from a direction in which high CH₄ emissions occur, for example an area of intensive agriculture. For winds from that direction, the observations would show peak CH₄ concentrations. The tracer representing agricultural emissions will show a comparable peak for winds from this direction. However, waste sources might not be located in this direction from the measurement site. The peak in the CH₄ concentration visible in the observations and the agricultural tracer, will not be visible in the waste tracer. The influence of the wind direction on the CH₄ concentration will be further discussed in section 4.3.

In Cabauw, the excess CH₄ concentration of agriculture and energy correlate best to the observations. In Cabauw, several tracers have a weaker correlation with the observations than in Lutjewad. The different spatial distribution of emission sources around Cabauw might cause lower correlation coefficients for the tracers. At Lutjewad almost all CH₄ sources are located to the south of the measurement location. For this reason different sources around Lutjewad will be more clustered in the same direction relative to Lutjewad, than the sources around Cabauw. At Cabauw CH₄ sources are located in all directions. Fewer of the smaller sources will be located in the wind direction for which CH₄ concentrations peak at Cabauw. This might cause the lower correlation coefficients for small CH₄ sources at Cabauw. Another reason could be the underestimation of emissions from some subgroups in Cabauw. This would be in line with the underestimation of the average CH₄ concentration in Cabauw. An unexpected result is that the excess CH₄ concentration from refineries emissions in Cabauw has no correlation with the variability in the observations, while the correlation is fairly high in Lutjewad. This despite the fact that there are more emissions from refineries around Cabauw, especially from the harbor of Rotterdam, than around Lutjewad. This might be a result of the refineries, located to the west of Cabauw, not being located in the direction of high

(agricultural) CH₄ emission, from the east of Cabauw. This effect is further discussed in section 4.3.

4.1.4 Correlation per month

On a monthly basis the correlation coefficients between simulated and observed CH₄ concentrations show large differences (see table 4 and 5). Almost all tracers show a relatively high or a relatively low correlation for the same months. For example, in Lutjewad in February, April and to an extent August, relatively high correlation coefficients are found for most tracers. On the other hand, in January and December relatively low correlation coefficients are found for most tracers in Lutjewad. In January and December the observations have large data gaps. Both months only have 2 weeks of observation, meaning the correlation coefficient is based on fewer data points than it is in other months. This might cause the relatively bad correlation for these two months. The same holds in November and December in Cabauw. However, in February there is as well only 2 weeks of observational data is available. This low amount of used data points for determining the correlation coefficient, results in February in relatively high correlation coefficients. Apart from this, in April and to an extent in August, relatively high correlation coefficients are found. There are no large gaps in the observational data for these months. An explanation for the relatively high correlation in April, both in Lutjewad and Cabauw, can be the lack of large peaks in the methane concentration during this month (see figure 8). In April the lowest variability in the observed CH₄ concentration is found compared to the other months. From the graphs in figure 8 it can be seen that the simulated concentration follows most peaks very well during this month.

4.2 Diurnal cycle of methane concentration

The results of the diurnal cycle of the methane concentrations showed an underestimation of the diurnal range in methane concentration by the simulations with the WRF-Chem model (figure 9 and 10). Especially in spring and summer the observations show a diurnal range in the methane concentration up to 150 ppb in Lutjewad and 200 ppb in Cabauw, while that of the simulation is less than 50 ppb. In January and December there are no clear diurnal cycles for the observations and simulations. The diurnal range in the observations in Lutjewad intensified from February to September and decreased thereafter. In Cabauw the diurnal range decreases after August. The simulation in Lutjewad and Cabauw shows an almost constant diurnal cycle from February to November, with a diurnal range of about 50 ppb. In Lutjewad the observations in spring and summer have a diurnal range that is up to 3 times the diurnal range shown in the simulations. In Cabauw the observed diurnal range is even up to 4 times the simulated diurnal range in methane concentration. The diurnal range in the observations in Cabauw in 2017 is in good agreement with the average observed diurnal range in Cabauw between 1992-2010 (Vermeulen et al., 2011).

The implementation of diurnal variability in the emissions of some tracers in a second simulations, did not cause major changes in the diurnal cycle in the simulated methane concentration. At Cabauw the difference between the first and second run is stronger than in Lutjewad. Although the shape of the

diurnal cycle changed slightly in the second run, overall the discrepancy in the diurnal range between observations and the simulation stayed the same. A likely cause of this discrepancy is that there is no diurnal variability implemented in the emission of the largest sources, agriculture and waste. These were not implemented because no diurnal multiplication factors were available for most important agricultural emission (Bultjes et al., 2003). Another study (Amon et al., 2001) showed a significant diurnal variability in enteric fermentation by cows, the largest agricultural source of methane. Agricultural CH₄ emissions are the largest source of methane in the Netherlands. Implementing a diurnal variability in the agricultural emission input for the simulations, should alter the diurnal variability in the simulated CH₄ concentration substantially. This is an important aspect for further research.

4.2.1 Boundary layer height

In the search for an explanation for the difference in the diurnal range between simulated and observed methane concentrations, the boundary layer height (BLH) was analyzed. The results in figure 11 showed that the simulations constantly underestimated the height of the boundary layer by 200-250 meters. Furthermore the phase of the diurnal cycle is slightly shifted in the simulations. The minimum and maximum in the BLH occurs several hours earlier in the simulation than in the observations. Despite these differences, the diurnal range of the BLH is about the same for the simulation as it is for the observations. The relative night and day ratio in the simulations is even larger than observed. In the summer the BLH is 3 to 4 times higher in the afternoon than it is during nighttime. The observations only show an afternoon BLH of double the nighttime BLH during the summer months. From this would be expected that the diurnal range in the CH₄ concentration would be higher in the simulations than in the observations. The opposite is found in the analysis. The diurnal variability in the simulated BLH does not seem to have the correct influence on the diurnal variability in the simulated CH₄ concentration. The timing of the diurnal cycle in the CH₄ concentration still matches that of the boundary layer height, i.e. the nighttime peaks coincide. For this reason it is very likely the boundary layer height is determining the diurnal cycle in the CH₄ concentration. A more extensive analysis on the correlation between the boundary layer height and the CH₄ concentration would be needed to draw solid conclusions. Difficulties with simulating the correct correlation between the variability in diurnal BLH and diurnal CH₄ concentration in WRF-Chem are also encountered in other studies (Kretschmer et al., 2014, Shi et al., 2020). Kretschmer et al., (2014) showed large biases of the BLH in WRF-Chem during nighttime.

A trustworthy reproduction of the diurnal variability in the CH₄ concentration by the WRF-Chem model is important for research on the variability of CH₄ emissions during short periods. For example to investigate and simulate the diurnal variability in the CH₄ emissions from specific sectors. Further analysis could also investigate whether there is better agreement with the observed CH₄ concentration during nighttime or during daytime. It is expected from earlier studies that especially the nighttime CH₄ concentrations are underestimated and daytime CH₄ concentration are in good agreement with the observations (Kretschmer

et al., 2014). This would also explain the on average underestimated CH₄ concentration in the simulations, shown in table 2.

4.3 Effect of wind direction on tracer concentration

The categorization of the methane emissions in many subgroups by the RIVM inventory, made it possible to research the effect of the emissions from these individual subgroups on the total methane concentration. As explained in the introduction section, the wind direction is expected to influence the magnitude of the excess methane concentration for every tracer. Peaks in methane concentration when wind is blowing from a certain direction, might point towards individual emission sources. Comparing this with the relative observed excess methane concentration, gives insight in the influence of individual sources on the observed methane concentration. First, the 24-hours averaged simulated wind direction during 2017 was compared with the observations. On average the simulated wind direction in Lutjewad and Cabauw differs by approximately 40 degrees from the observed wind direction.

The normalized excess methane concentration is determined for every tracer, for 8 wind directions. In Lutjewad, the total of all tracers showed the highest excess concentration for wind from the south-southeast. This is also the case for the observations. The observations showed an excess CH₄ concentration of 3 times the average excess CH₄ concentration when the wind was blowing from the south-southeast. However, the simulated excess CH₄ concentration was only 1.7 times the average excess concentration for wind blowing from the south-southeast. At Cabauw, the total simulated excess CH₄ concentration was the highest when wind was blowing from the east-northeast. The observations showed the highest excess concentration for winds that were blowing from the east-southeast and south-southeast. The wind direction for which the highest excess concentration occurred in the simulation, is turned 45-90 degrees counterclockwise with respect to the observations. Apart from this difference in direction, the relative excess CH₄ concentration also differs. For the simulation the highest excess concentration was 1.4 times the average excess concentration. The observations showed excess concentrations that were 1.8 times the average excess concentrations, for the wind direction east-southeast and south-southeast. For Lutjewad and to a lesser extent for Cabauw, the simulation underestimated the influence of the wind direction on the excess methane concentration. A reason for this underestimation could be the underestimation of CH₄ emissions, especially in the direction for which the highest excess concentration is found. Another reason might be the low amount of data point used per wind direction for this analysis. Especially for eastern wind directions only 100 to 200 data points could be used for which the simulated and observed wind blew from the same direction. Only a short amount of time is covered by these data points, compared to the full simulation period.

With the use of the wind roses for the individual tracers, the effect of individual CH₄ sources on the excess methane concentration in Lutjewad and Cabauw can be investigated. For example, the energy tracer in Lutjewad shows excess CH₄ concentrations more than double the average for wind from the south-southeast. Figure 22 (see appendix) demonstrates that in the south-southeastern direction from Lutjewad

large emissions sources are located. These large emissions are from the natural gas exploitation in the east of the Groningen province. Another example is the excess CH_4 concentration of the tracer representing emissions from refineries near Cabauw. For wind from the west-southwest direction, the excess CH_4 concentration of the refineries tracers is 2.3 times the average excess CH_4 concentration. Figure 21 (see appendix) shows that CH_4 refinery sources are located in the west-southwest direction from Cabauw. For most of the tracers the largest CH_4 sources are found in the direction of the wind for which the excess CH_4 concentration is the highest. The maps of emissions data for all individual tracers can be found in section 7.2.

It should also be noted that the wind direction for which the excess CH_4 concentration is highest might not coincide with the direction in which the largest CH_4 sources are located. One cause for peak events in CH_4 concentration are calm weather conditions. These calm weather conditions might occur more frequently when wind blows from a specific direction. The wind direction for which the excess CH_4 concentration is the highest might coincide with the wind direction for which calm weather conditions occur most frequently. In Lutjewad this seems to be the case because most tracers have the highest excess CH_4 concentrations for wind blowing from a south-southeastern direction. Not all of these tracers have their largest sources located in this direction. In Cabauw the differences in the magnitude of the excess CH_4 concentration per wind direction are smaller. For this reason it is hard to draw solid conclusions whether calm weather conditions or large emissions sources are the cause for the high excess CH_4 concentration of tracers in a particular wind direction. Further analysis would be needed to determine the effect of these calm weather conditions on the wind direction for which excess CH_4 are highest.

4.4 Limitations

4.4.1 The WRF-Chem model

The preparation of the WRF-Chem model simulations and learning its features was a very time demanding process. As a consequence only a short amount of time was left for conducting and analyzing the simulations. The aim was to conduct 1 km x 1 km resolution simulations of the methane concentration on the domain of the Netherlands for the full year of 2017, with a maximum run time of 1 week. This turned out to be unfeasible, because such a run would have a run time of several months. The compromise was a run with a resolution of 3 km x 3 km on the domain of the Netherlands. With these settings, the run time was still two weeks. This long run time was mainly caused by the time steps in the simulation, which had to be very small for runs with a small grid size. The advised ideal time step was 6 times the grid size of the coarse domain. However, experience learned that the time step could not be larger than 3 times the grid size of the coarse domain. Even with such a small time step, there still occurred several computer errors with unknown reason during the simulations. Fortunately, the runs could be restarted with an even smaller time step just before the moment the error occurred. Considering all, the run time of the WRF-Chem model

is too long for conducting simulations with such a high resolution for a time period of one year or more on a domain of 85000 km². Especially when the research time is limited, a run time of 2 weeks makes it hard to optimize the simulations.

4.4.2 Input data

The emission inventory for the Netherlands is of very high spatial resolution. This made it possible to conduct high resolution simulations. However, the emission data was only provided as the yearly emission per subgroup. No information on variability in the emissions throughout 2017 was available. This lack of variability, potentially causes discrepancies in methane concentration between the simulations and observations. For the coarse domain, the EDGAR emission data was used. The most recent available emission inventory from EDGAR was for 2015. Emissions in 2015 were possibly different from those in 2017. Moreover, this EDGAR emission inventory is categorized in different subgroups than the RIVM inventory. To use this inventory for the coarse domain, the EDGAR subgroups had to be matched with the RIVM subgroups. However, not enough information was available to match all EDGAR subgroups to the RIVM subgroups in a correct way. Due to this inability to match all subgroups, certain tracers had no emissions in the simulated outer domain. This led to a lower quality of the representation of methane emission from outside of the Netherlands. For the second run that was conducted to investigate the diurnal cycle in the methane concentration, hourly multiplication factors for methane emissions were used. These multiplication factors are based on general variability in activity of several anthropogenic processes. These factors are not specifically generated for methane emission. Insights in the diurnal cycles of methane emission by different sources are still not thorough enough. More research in optimizing the emission inventory for these diurnal cycles in the methane emission can give better insight in the performance of the WRF-Chem simulation on diurnal time scales.

4.4.3 Measurement data

The available measurement data for CH₄ concentration in the Netherlands was sparse. Only two continuous measurement sites are located in the Netherlands that were operational during most of 2017. A consequence was that the simulation output could only be tested for these two locations. Moreover, both sites are located in the middle of an agricultural area. These two sites are not enough to give full insight in the performance of the model for the whole of the Netherlands. Furthermore, a better testing on the emission inventory could be done with a larger amount of measurement sites. Using more measurement sites to compare the simulations with, would give the opportunity to conduct a statistical analysis on the overall performance of the WRF-Chem model in simulations of CH₄ concentrations.

4.5 Recommendations for further research

The study conducted for this master project was an exploratory research. In this case this means that it is investigated whether WRF-Chem is a suitable model to simulate high resolution CH₄ concentrations in the Netherlands. Despite the long run time, this model has proven to be suitable for these kind of simulations. This means many research questions can be investigated with the use of this WRF-Chem model. The limitations discussed in the previous subsection, form the basis for several possible future studies. 1) The simulations with the WRF-Chem model could be compared with measurement data from more locations. Maybe regional measurement campaign data can be used to analyze shorter periods. Furthermore, for the longer term, more continuous measurements of methane concentration in the Netherlands could be conducted. This could give better insight in the methane emissions of the whole of the Netherlands. In that case the simulations can be thoroughly compared with measurements. 2) Future research can be on the influence of local sources. With the use of a mobile CH₄ measurement instrument, emissions from local sources can be captured better. With a better insight in these local sources, the discrepancy between simulations and observations during peak events can possibly be explained. This kind of research on local CH₄ emissions with a mobile measurement instrument has recently been conducted for emissions in large cities (Maazallahi et al., 2020). 3) Research could focus on conducting simulations with higher spatial resolutions (1 km x 1 km). Smaller domains should be chosen to reduce the run time. Small domains covering the area around Lutjewad and Cabauw might be chosen. Simulations conducted with this 1 km x 1 km resolution might capture the local plume emissions better and therefore, represent the peak concentration events better. 4) Further research could focus on finding a cause for the underestimated diurnal range in the simulated methane concentrations.

5 Conclusion

This study aimed to compare high resolution simulations of the methane concentration in the Netherlands, to *in situ* measurements. For conducting high resolution simulations of methane concentration, the WRF-Chem model was used. Methane emissions from the RIVM emission inventory are used as input with a 3 km x 3 km grid size on a rectangular domain covering all of the Netherlands. The output of this simulation is compared with measurements in Lutjewad and Cabauw during 2017. The research questions stated in section 1.1 are answered throughout this conclusion section.

How well does the simulation without diurnal or season cycle in the emission correspond to the measurements in Lutjewad and Cabauw?

The simulations showed a good agreement with the observation for the occurrence of peaks in the CH₄ concentration. Most peaks that occur in the observed methane concentration are also represented by the simulations. However, the magnitude of the methane concentrations is significantly lower in the simulations. This underestimation is most likely caused by the average methane emissions over an area

of 3 km x 3 km being taken as input for the simulations. With taking this average emission, plumes from emission sources will be more spread out and therefore less concentrated in the simulations than they are in reality. Local accumulation of CH₄ during peak events, might therefore be less well captured in the simulations. The CH₄ concentration in Cabauw is underestimated for most of the year. This might point to some underestimated or missing sources in the emission inventory.

The correlation between the simulated and observed excess CH₄ concentrations is determined per month for every tracer. In certain months most tracers showed relatively low correlation with the observations and in other months most tracers showed relatively high correlation with the observations. The months in which relatively low correlations were found are the months with large gaps in the observational data. Due to the small amount of observational data in these months, the correlation coefficient is based on a short period of time which does possibly not represent the whole month. In April most tracers show the highest correlation with the observations compared to other months, both in Lutjewad and Cabauw. In April the variability in the observed methane concentration is lowest, both in Lutjewad and Cabauw. Due to this lower variability in the observations, the simulations represent the variability in this month best.

Can the implementation of diurnal cycles on the emission improve the correspondence in diurnal trend between simulations and measurements, and if not can other causes be addressed?

The observations in Lutjewad showed a 3 times larger diurnal range, of 150 ppb, in the methane concentration for the summer months, than the simulation. In Cabauw, the observed diurnal range is, with 225 ppb, even more than 4 times higher than the simulated diurnal range, during the summer. No significant diurnal cycle occurred in the observations and simulations during winter time. Implementing diurnal variability in the methane emissions of several sources, only resulted in minor changes to the diurnal cycle in the simulated methane concentration. An expected cause of the difference in diurnal range the CH₄ concentration between simulation and observations was a possible discrepancy in the diurnal variability of the boundary layer height, between observations and the simulation. However, the diurnal range of the boundary layer height in the simulations did not show differences with the observations that were large enough to explain the difference in the diurnal range of the methane concentration. The diurnal ratio of daytime BLH and nighttime BLH during the summer months was higher in the simulations than in the observations. This result implies that that the diurnal range in the simulations should be higher than in the observations. However, the opposite is found in this study.

Does the wind direction have impact on the excess concentration of the tracers detected at the measurement locations?

In Lutjewad, most tracers had excess CH₄ concentration that were higher than average when the wind blew from southern directions. This is consistent with the observed methane concentrations. Both in the simulations and the observation, the total excess CH₄ concentration showed the highest excess methane concentrations for wind from the south-southeastern direction. However, the simulations showed for this wind direction a concentration of 1.7 times the average methane concentration, while the observations

showed a methane concentration of 3 times the average observed concentration. In Cabauw the simulated total CH₄ concentration of all tracers showed the highest excess concentrations for wind blowing from the east-northeast. The simulated methane concentration for this wind direction was 1.4 times the average simulated methane concentration. The observations showed the highest excess concentration when the wind blew from east-southeastern and south-southeastern directions. For these wind directions the observed excess methane concentration is 1.8 times the average excess methane concentration. Both in Lutjewad and Cabauw the influence of the wind direction on the magnitude of the excess methane concentration is underestimated by the simulation. This can be caused by underestimated local methane emission. Another reason could be the poor representation of plume emission using a resolution of 3 km x 3 km.

Can the observed methane concentration in Lutjewad and Cabauw be reproduced by model simulations with the use of a high resolution methane emission inventory as input in the WRF-Chem model?

In conclusion it can be stated that, despite the relatively long run time, the WRF-Chem model was suitable for performing high resolution simulations of methane concentrations in the Netherlands. Variability in the CH₄ concentration at Lutjewad and Cabauw on time scales of weeks and months is fairly well reproduced by the model simulations. Simulations with a higher spatial resolutions might improve the reproduction of the maximum CH₄ concentration during peak events. The variability in CH₄ concentration on a diurnal time scale is not well represented by the WRF-Chem simulations. Further research should be conducted on the discrepancies in the variability in diurnal methane concentration between the WRF-Chem simulations and the observations. Resolving these discrepancies will increase the accuracy with which the effect of methane emissions on the methane concentration can be determined.

6 References

- Amon, B., Amon, T., Boxberger, J., & Alt, C. (2001). Emissions of NH₃, N₂O and CH₄ from dairy cows housed in a farmyard manure tying stall (housing, manure storage, manure spreading). *Nutrient Cycling in Agroecosystems*, 60, 103–113. <https://doi.org/10.1023/A:1012649028772>
- Bachelet, D., & Neue, H. U. (1993). Methane emissions from wetland rice areas of Asia. *Chemosphere*, 26(1), 219–237. [https://doi.org/10.1016/0045-6535\(93\)90423-3](https://doi.org/10.1016/0045-6535(93)90423-3)
- Beck, V., Gerbig, C., Koch, T., Bela, M. M., Longo, K. M., Freitas, S. R., Kaplan, J. O., Prigent, C., Bergamaschi, P., & Heimann, M. (2013). WRF-Chem simulations in the Amazon region during wet and dry season transitions: Evaluation of methane models and wetland inundation maps. *Atmospheric Chemistry and Physics*, 13(16), 7961–7982. <https://doi.org/10.5194/acp-13-7961-2013>
- Beck, V., Koch, T., Kretschmer, R., Marshall, J., Ahmadov, R., Gerbig, C., Pillai, D., & Heimann, M. (2011). *The WRF Greenhouse Gas Model (WRF-GHG)* (No. 25). Max Planck Institute for Biogeochemistry.
- Bousquet, P., Ciais, P., Miller, J. B., Dlugokencky, E. J., Hauglustaine, D. A., Prigent, C., Van der Werf, G. R., Peylin, P., Brunke, E.-G., Carouge, C., Langenfelds, R. L., Lathière, J., Papa, F., Ramonet, M., Schmidt, M., Steele, L. P., Tyler, S. C., & White, J. (2006). Contribution of anthropogenic and natural sources to atmospheric methane variability. *Nature*, 443(7110), 439–443. <https://doi.org/10.1038/nature05132>
- Bridgman, S. D., Cadillo-Quiroz, H., Keller, J. K., & Zhuang, Q. (2013). Methane emissions from wetlands: Biogeochemical, microbial, and modeling perspectives from local to global scales. *Global Change Biology*, 19(5), 1325–1346. <https://doi.org/10.1111/gcb.12131>
- Builtjes, P. J. H., van Loon, M., Schaap, M., Teeuwisse, S., Visschedijk, A. J. H., & Bloos, J. P. (2003). *Project on the modelling and verification of ozone reduction strategies: Contribution of TNO-MEP, TNO-report. MEP-R2003/166*, Apeldoorn, The Netherlands.
- Chen, Y.-H., & Prinn, R. G. (2006). Estimation of atmospheric methane emissions between 1996 and 2001 using a three-dimensional global chemical transport model. *Journal of Geophysical Research: Atmospheres*, 111(D10). <https://doi.org/10.1029/2005JD006058>
_eprint: <https://agupubs.onlinelibrary.wiley.com/doi/pdf/10.1029/2005JD006058>
- Compedium, voor de Leefomgeving. (2020, September 2). *Emissies broeikasgassen, 1990-2018 | Compedium voor de Leefomgeving*. Retrieved September 2, 2020, from <https://www.clo.nl/indicatoren/nl016535-broeikasgasemissies-in-nederland>
- Conrad, R. (2002). Control of microbial methane production in wetland rice fields. *Nutrient Cycling in Agroecosystems*, 64(1), 59–69. <https://doi.org/10.1023/A:1021178713988>
- de Haij, M., Wauben, W., & Baltink, H. K. (2017). *Continuous mixing layer height determination using the LD-40 ceilometer: A feasibility study*. Royal Netherlands Meteorological Institute (KNMI).

- Dlugokencky, E. J., Houweling, S., Bruhwiler, L., Masarie, K. A., Lang, P. M., Miller, J. B., & Tans, P. P. (2003). Atmospheric methane levels off: Temporary pause or a new steady-state? *Geophysical Research Letters*, 30(19). <https://doi.org/10.1029/2003GL018126>
_eprint: <https://agupubs.onlinelibrary.wiley.com/doi/pdf/10.1029/2003GL018126>
- ECMWF. (2020a, April 29). *ECMWF | CAMS Greenhouse Gases Flux Inversions*. Retrieved April 29, 2020, from <https://apps.ecmwf.int/datasets/data/cams-ghg-inversions/>
- ECMWF. (2020b, March 23). *ERA-Interim*. Retrieved March 23, 2020, from <https://www.ecmwf.int/en/forecasts/datasets/reanalysis-datasets/era-interim>
- Etheridge, D. M., Steele, L. P., Francey, R. J., & Langenfelds, R. L. (1998). Atmospheric methane between 1000 A.D. and present: Evidence of anthropogenic emissions and climatic variability. *Journal of Geophysical Research: Atmospheres*, 103(D13), 15979–15993. <https://doi.org/10.1029/98JD00923>
- European Commission. (2020a, February 18). *European commission, methane gas emissions*. Retrieved February 18, 2020, from https://ec.europa.eu/energy/topics/oil-gas-and-coal/methane-gas-emissions_en
- European Commission. (2020b, April 25). *JRC EDGAR - European Commission*. Retrieved August 28, 2020, from <https://data.jrc.ec.europa.eu/collection/edgar>
- Fruman, K. (2016). *ECN Publication ECN-E-16-031*. Retrieved August 28, 2020, from <http://www.ecn.nl/publications/ECN-E--16-031>
- Hong, S.-Y. (2010). A new stable boundary-layer mixing scheme and its impact on the simulated East Asian summer monsoon. *Quarterly Journal of the Royal Meteorological Society*, 136(651), 1481–1496. <https://doi.org/10.1002/qj.665>
_eprint: <https://rmets.onlinelibrary.wiley.com/doi/pdf/10.1002/qj.665>
- Hong, S.-Y., & Pan, H.-L. (1996). Nonlocal Boundary Layer Vertical Diffusion in a Medium-Range Forecast Model. *Monthly Weather Review*, 124(10), 2322–2339. [https://doi.org/10.1175/1520-0493\(1996\)124<2322:NBLVDI>2.0.CO;2](https://doi.org/10.1175/1520-0493(1996)124<2322:NBLVDI>2.0.CO;2)
- Kai, F. M., Tyler, S. C., Randerson, J. T., & Blake, D. R. (2011). Reduced methane growth rate explained by decreased Northern Hemisphere microbial sources. *Nature*, 476(7359), 194–197. <https://doi.org/10.1038/nature10259>
- Khalil, M. a. K., & Rasmussen, R. A. (1983). Sources, sinks, and seasonal cycles of atmospheric methane. *Journal of Geophysical Research: Oceans*, 88(C9), 5131–5144. <https://doi.org/10.1029/JC088iC09p05131>
_eprint: <https://agupubs.onlinelibrary.wiley.com/doi/pdf/10.1029/JC088iC09p05131>
- Kirschke, S., Bousquet, P., Ciais, P., Saunois, M., Canadell, J. G., Dlugokencky, E. J., Bergamaschi, P., Bergmann, D., Blake, D. R., Bruhwiler, L., Cameron-Smith, P., Castaldi, S., Chevallier, F., Feng, L., Fraser, A., Heimann, M., Hodson, E. L., Houweling, S., Josse, B., ... Zeng, G. (2013). Three decades of global methane sources and sinks. *Nature Geoscience*, 6(10), 813–823. <https://doi.org/10.1038/ngeo1955>

- Kort, E. A., Frankenberg, C., Costigan, K. R., Lindenmaier, R., Dubey, M. K., & Wunch, D. (2014). Four corners: The largest US methane anomaly viewed from space. *Geophysical Research Letters*, *41*(19), 6898–6903. <https://doi.org/10.1002/2014GL061503>
- Kretschmer, R., Gerbig, C., Karstens, U., Biavati, G., Vermeulen, A., Vogel, F., Hammer, S., & Totsche, K. U. (2014). Impact of optimized mixing heights on simulated regional atmospheric transport of CO₂. *Atmospheric Chemistry and Physics*, *14*(14), 7149–7172. <https://doi.org/10.5194/acp-14-7149-2014>
- Lelieveld, J., Gromov, S., Pozzer, A., & Taraborrelli, D. (2016). Global tropospheric hydroxyl distribution, budget and reactivity. *Atmospheric Chemistry and Physics*, *16*(19), 12477–12493. <https://doi.org/10.5194/acp-16-12477-2016>
- Lu, X., Zhang, L., & Shen, L. (2019). Meteorology and Climate Influences on Tropospheric Ozone: A Review of Natural Sources, Chemistry, and Transport Patterns. *Current Pollution Reports*, *5*(4), 238–260. <https://doi.org/10.1007/s40726-019-00118-3>
- Maazallahi, H., Fernandez, J. M., Menoud, M., Zavala-Araiza, D., Weller, Z. D., Schwietzke, S., von Fischer, J. C., Denier van der Gon, H., & Röckmann, T. (2020). Methane mapping, emission quantification and attribution in two European cities; Utrecht, NL and Hamburg, DE. *Atmospheric Chemistry and Physics Discussions*, 1–30. <https://doi.org/10.5194/acp-2020-657>
- Ministerie van Infrastructuur en Waterstaat. (2017). *Netherlands national report on Black Carbon and Methane emissions*. Retrieved August 28, 2020, from <https://www.ccacoalition.org/en/resources/netherlands-national-report-black-carbon-and-methane-emissions>
- Myhre, G., Shindell, D., Bréon, F.-M., Collins, W., Fuglestedt, J., Huang, J., Koch, D., Lamarque, J.-F., Lee, D., Mendoza, B., Nakajima, T., Robock, A., Stephens, G., Zhang, H., Aamaas, B., Boucher, O., Dal-søren, S. B., Daniel, J. S., Forster, P., ... Shine, K. (2013). 8 Anthropogenic and Natural Radiative Forcing, 82.
- NOAA Research, US Department of Commerce. (2020). *Global Monitoring Laboratory - Carbon Cycle Greenhouse Gases*. Retrieved August 28, 2020, from https://www.esrl.noaa.gov/gmd/ccgg/trends_ch4/
- Park, S. K., Lim, S., & Zupanski, M. (2015). Forecast error covariance structure in coupled atmosphere–chemistry data assimilation. *Geoscientific Model Development*, *8*, 1315–1320. <https://doi.org/10.5194/gmd-8-1315-2015>
- Reum, F., Florentie, L., Peters, W., Dogniaux, M., Crevoisier, C., Sic, B., & Houweling, S. (2020). Performance of upcoming CO₂ monitoring satellites in the new high-resolution inverse model CTDAS-WRF, 22, 19293. Retrieved August 28, 2020, from <http://adsabs.harvard.edu/abs/2020EGUGA..2219293R>
- Rijksuniversiteit Groningen. (2020, May 14). *Station Lutjewad | Carbon cycle - Atmosphere | Rijksuniversiteit Groningen*. Retrieved August 28, 2020, from <https://www.rug.nl/research/centre-for-isotope-research/research-and-projects/main-research/carbon-cycle-atmosphere/lutjewad/?lang=en>
- RIVM. (2019). Greenhouse gas emissions in the Netherlands 1990–2017, National Inventory Report 2019, 420. <https://www.rivm.nl/bibliotheek/rapporten/2019-0020.pdf>

- RIVM, Emissieregistratie. (2020, September 15). *Emissieregistratie*. Retrieved September 15, 2020, from <http://www.emissieregistratie.nl/erpubliek/content/explanation.nl.aspx#kwaliteit>
- Saha, C., Ammon, C., Berg, W., Loebsin, C., Fiedler, M., Brunsch, R., & Bobruzki, K. (2013). The effect of external wind speed and direction on sampling point concentrations, air change rate and emissions from a naturally ventilated dairy building. *Biosystems Engineering*, *114*, 267–278. <https://doi.org/10.1016/j.biosystemseng.2012.12.002>
- Saunio, M., Stavert, A. R., Poulter, B., Bousquet, P., Canadell, J. G., Jackson, R. B., Raymond, P. A., Dlugokencky, E. J., Houweling, S., Patra, P. K., Ciais, P., Arora, V. K., Bastviken, D., Bergamaschi, P., Blake, D. R., Brailsford, G., Bruhwiler, L., Carlson, K. M., Carrol, M., ... Zhuang, Q. (2020). The Global Methane Budget 2000–2017. *Earth System Science Data*, *12*(3), 1561–1623. <https://doi.org/10.5194/essd-12-1561-2020>
- Savolainen, I., Monni, S., & Syri, S. (2009). THE MITIGATION OF METHANE EMISSIONS FROM INDUSTRIALIZED COUNTRIES CAN EXPLAIN THE ATMOSPHERIC CONCENTRATION LEVEL-OFF. *International Journal of Energy for a Clean Environment*, *10*(1-4). <https://doi.org/10.1615/InterJEnerCleanEnv.2011001603>
- Shi, Y., Hu, F., Xiao, Z., Fan, G., & Zhang, Z. (2020). Comparison of four different types of planetary boundary layer heights during a haze episode in Beijing. *Science of The Total Environment*, *711*, 134928. <https://doi.org/10.1016/j.scitotenv.2019.134928>
- Simpson, I. J., Sulbaek Andersen, M. P., Meinardi, S., Bruhwiler, L., Blake, N. J., Helmig, D., Rowland, F. S., & Blake, D. R. (2012). Long-term decline of global atmospheric ethane concentrations and implications for methane. *Nature*, *488*(7412), 490–494. <https://doi.org/10.1038/nature11342>
- Skamarock, W. C., Klemp, J. B., Dudhia, J., Gill, D. O., Barker, D. M., Duda, M. G., Huang, X.-y., Wang, W., & Powers, J. G. (2008). G.: A description of the Advanced Research WRF version 3. *NCAR Tech. Note NCAR/TN-475+STR*.
- van Doorn, E., Dhruva, B., Sreenivasan, K. R., & Cassella, V. (2000). Statistics of wind direction and its increments. *Physics of Fluids*, *12*(6), 1529–1534. <https://doi.org/10.1063/1.870401>
- Vermeulen, A., Hensen, A., Popa, E., Bulk, W., & Jongejan, P. (2011). Greenhouse gas observations from Cabauw Tall Tower (1992-2010). *Atmospheric Measurement Techniques*, *4*, 617–644.
- Villani, M. G., Bergamaschi, P., Krol, M., Meirink, J. F., & Dentener, F. (2010). Inverse modeling of European CH₄ emissions: Sensitivity to the observational network. *Atmospheric Chemistry and Physics*, *10*(3), 1249–1267. <https://doi.org/10.5194/acp-10-1249-2010>
- Walter, B. P., & Heimann, M. (2000). A process-based, climate-sensitive model to derive methane emissions from natural wetlands: Application to five wetland sites, sensitivity to model parameters, and climate. *Global Biogeochemical Cycles*, *14*(3), 745–765. <https://doi.org/10.1029/1999GB001204>

- Yacovitch, T. I., Neininger, B., Herndon, S. C., van der Gon, H. D., Jonkers, S., Hulskotte, J., Roscioli, J. R., & Zavala-Araiza, D. (2018). Methane emissions in the Netherlands: The Groningen field. *Elem Sci Anth*, 6(1), 57. <https://doi.org/10.1525/elementa.308>
- Yuval, Tritscher, T., Raz, R., Levi, Y., Levy, I., & Broday, D. M. (2020). Emissions vs. turbulence and atmospheric stability: A study of their relative importance in determining air pollutant concentrations. *Science of The Total Environment*, 733, 139300. <https://doi.org/10.1016/j.scitotenv.2020.139300>

7 Appendix

7.1 Tables of tracers

Table 6: The 13 different emissions groups defined in the RIVM emission inventory.

Tracer number	Emission source
1	Agriculture
2	Other industry
3	Chemical industry
4	Refineries
5	Energy
6	Traffic and transport
7	Consumers
8	Construction
9	Waste treatment
10	Water purification
11	Waste water
12	Trade
13	Nature

Table 7: The categorization of EDGAR emission groups into the 13 RIVM emissions groups as numbered in table 6.

Source group EDGAR	Source group RIVM
Power industry	5
Oil refineries and Transformation industry	4
Combustion for manufacturing	2
Aviation climbing&descent	6
Aviation cruise	6
Aviation landing&takeoff	6
Aviation supersonic	6
Road transportation	6
Railways, pipelines, off-road transport	6
Shipping	6
Energy for buildings	7
Fuel exploitation COAL	5
Fuel exploitation	5
Fuel exploitation OIL	5
Fuel exploitation GAS	5
Non-metallic minerals production	2
Chemical processes	3
Iron and steel production	2
Enteric fermentation	1
Manure management	1
Agricultural waste burning	1
Agricultural soils	1
Solid waste landfills	9
Solid waste incineration	9
Waste water handling	11
Fossil Fuel Fires	5

Table 8: Different diurnal multiplication factor per hour. The first row indicated the hour of the day. The first column is the number of the diurnal profile used to link the specific diurnal profiles to the tracers, see table 9. Note that this table is split into two tables, one from 00:00 - 11:00 and one from 12:00 - 23:00, for better visibility.

	00:00	01:00	02:00	03:00	04:00	05:00	06:00	07:00	08:00	09:00	10:00	11:00
1	0.79	0.72	0.72	0.71	0.74	0.8	0.92	1.08	1.19	1.22	1.21	1.21
2	0.38	0.36	0.36	0.36	0.37	0.5	1.19	1.53	1.57	1.56	1.35	1.16
3	0.75	0.75	0.78	0.82	0.88	0.95	1.02	1.09	1.16	1.22	1.28	1.3
4	0.5	0.35	0.2	0.1	0.1	0.2	0.75	1.25	1.4	1.5	1.5	1.5
5	0.19	0.09	0.06	0.05	0.09	0.22	0.86	1.84	1.86	1.41	1.24	1.2
6	1	1	1	1	1	1	1	1	1	1	1	1

	12:00	13:00	14:00	15:00	16:00	17:00	18:00	19:00	20:00	21:00	22:00	23:00
1	1.17	1.15	1.14	1.13	1.1	1.07	1.04	1.02	1.02	1.01	0.96	0.88
2	1.07	1.06	1	0.98	0.99	1.12	1.41	1.52	1.39	1.35	1	0.42
3	1.22	1.24	1.25	1.16	1.08	1.01	0.95	0.9	0.85	0.81	0.78	0.75
4	1.5	1.5	1.5	1.5	1.5	1.4	1.25	1.1	1	0.9	0.8	0.7
5	1.32	1.44	1.45	1.59	2.03	2.08	1.51	1.06	0.74	0.62	0.61	0.44
6	1	1	1	1	1	1	1	1	1	1	1	1

Table 9: The diurnal profile implemented for every tracers in the second simulation. The diurnal profile numbers from table 8 are use.

Tracer number	Emission source	Diurnal profile
1	Agriculture	6
2	Other industry	3
3	Chemical industry	4
4	Refineries	6
5	Energy	1
6	Traffic and transport	5
7	Consumers	2
8	Construction	6
9	Waste treatment	6
10	Water purification	6
11	Waste water	6
12	Trade	6
13	Nature	6

7.2 Maps of CH₄ emissions per tracer in the Netherlands

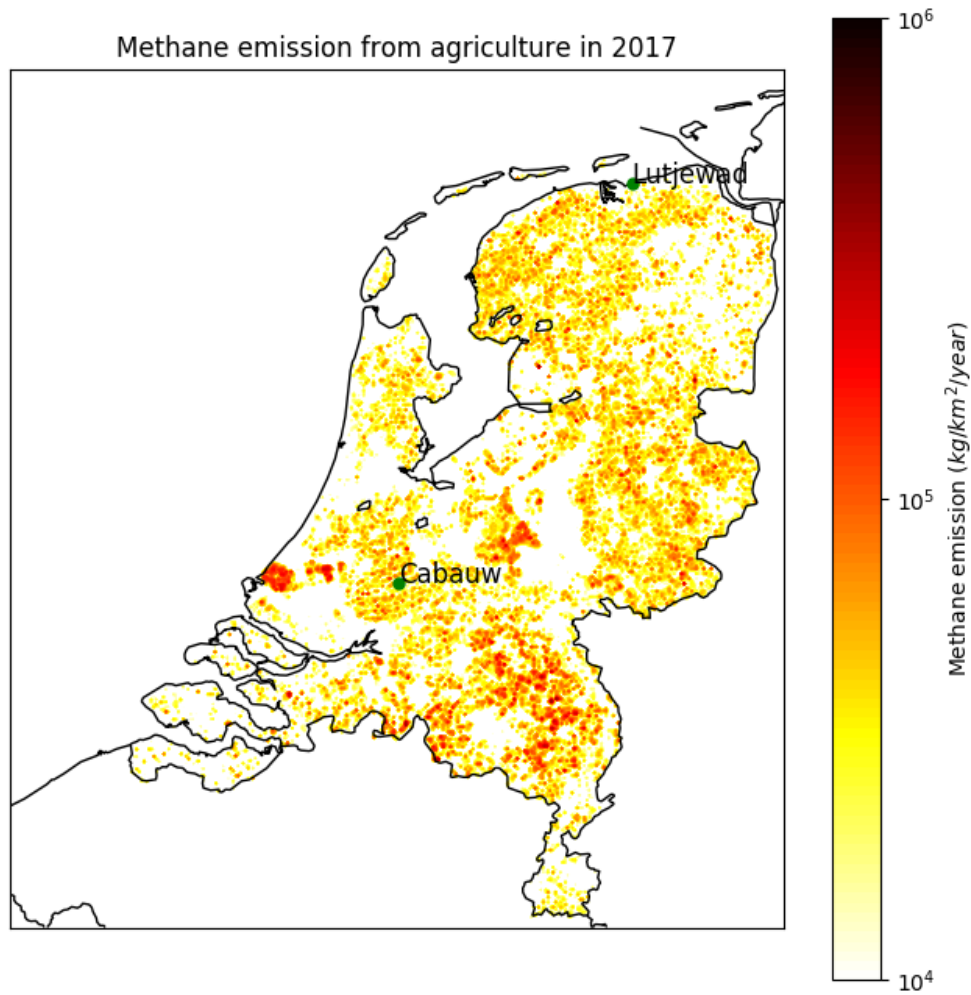


Figure 18: CH₄ emissions from the refineries in the Netherlands in 2017. Note that emissions smaller than 10⁴ kg/km²/year are not shown on the map.

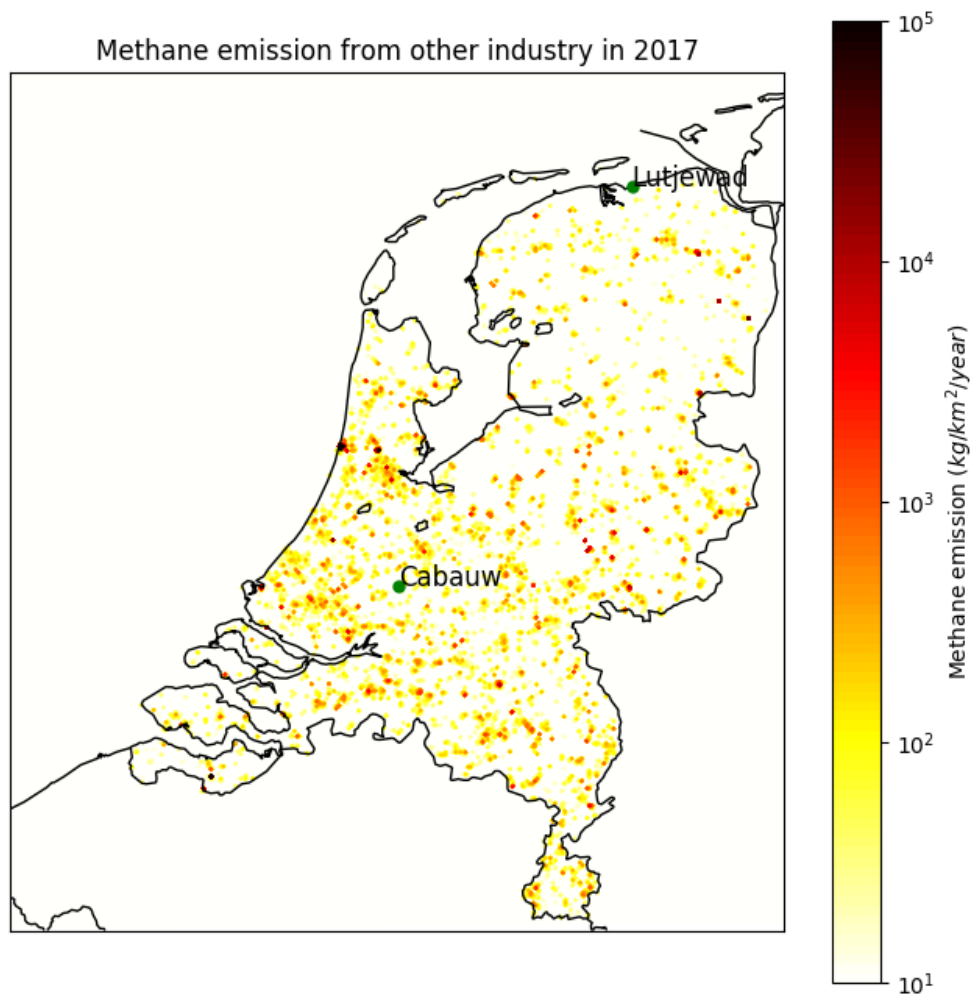


Figure 19: CH₄ emissions from the other industry in the Netherlands in 2017. Note that emissions smaller than 10^1 kg/km²/year are not shown on the map.

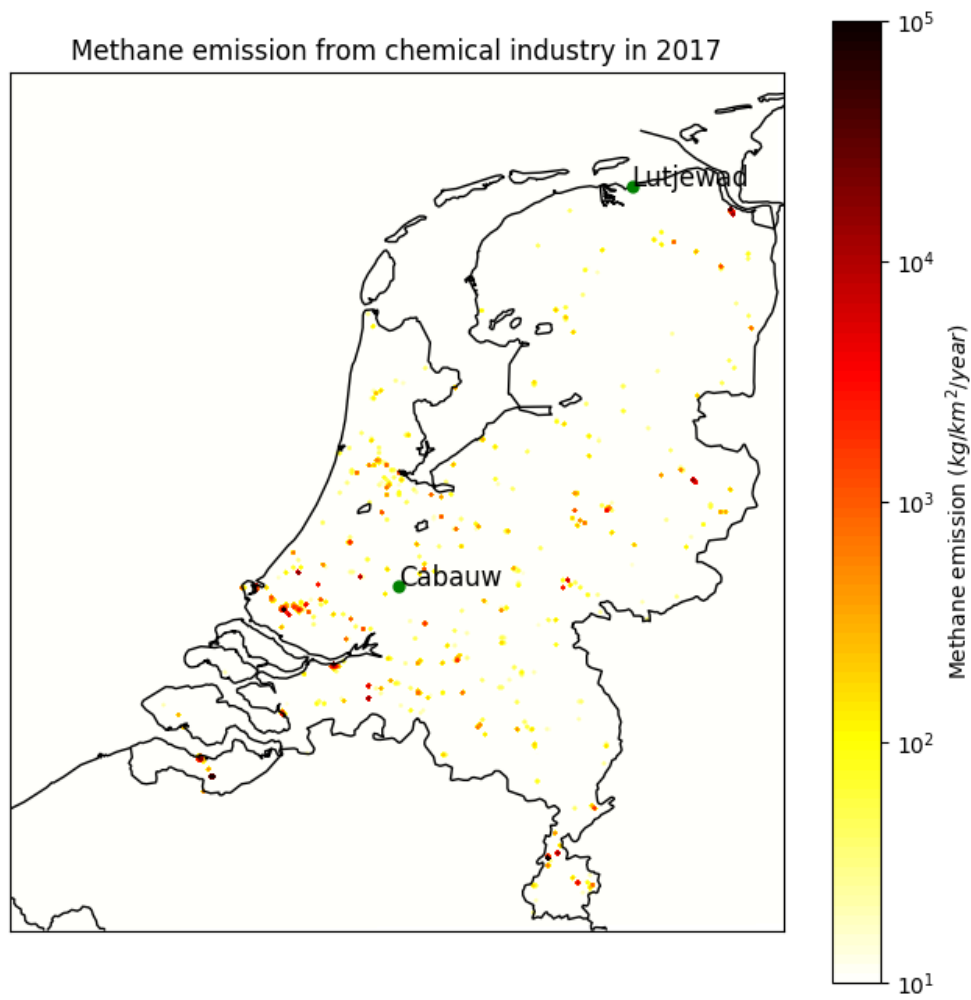


Figure 20: CH_4 emissions from the chemical industry in the Netherlands in 2017. Note that emissions smaller than 10^1 $\text{kg}/\text{km}^2/\text{year}$ are not shown on the map.

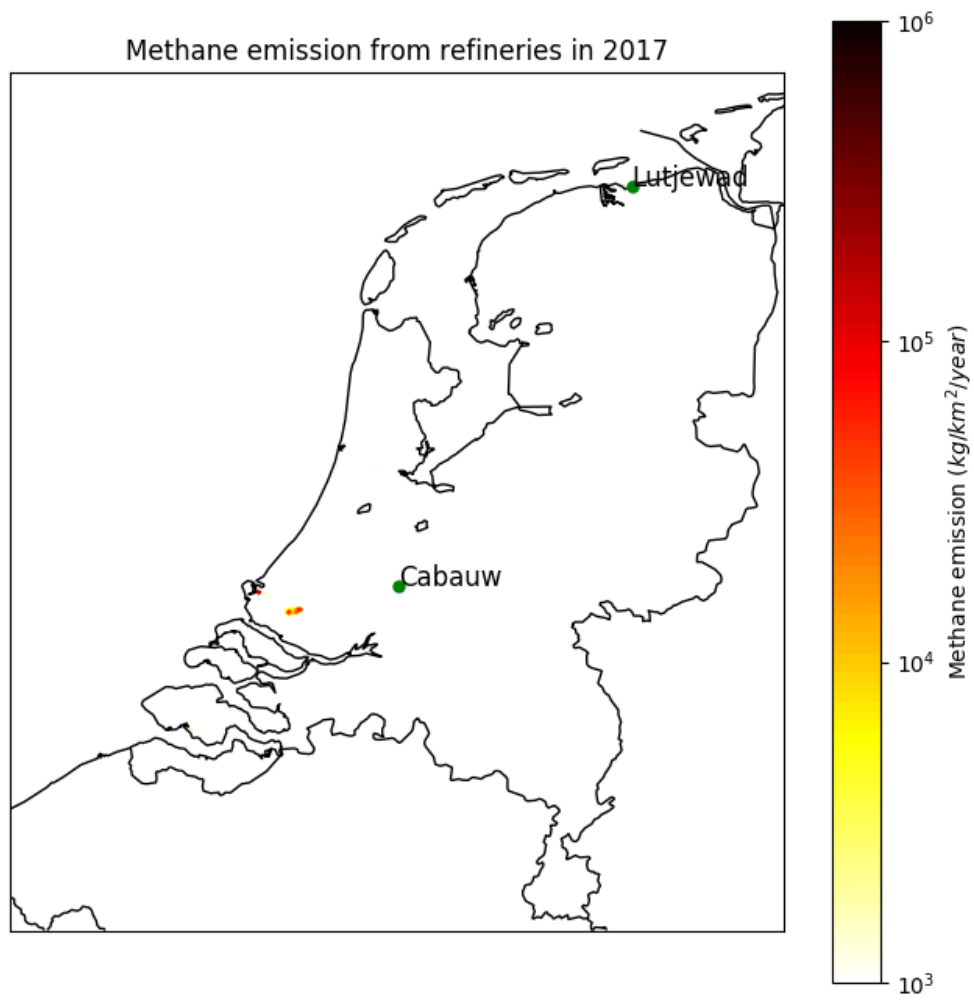


Figure 21: CH₄ emissions from the refineries in the Netherlands in 2017. Note that emissions smaller than 10³ kg/km²/year are not shown on the map.

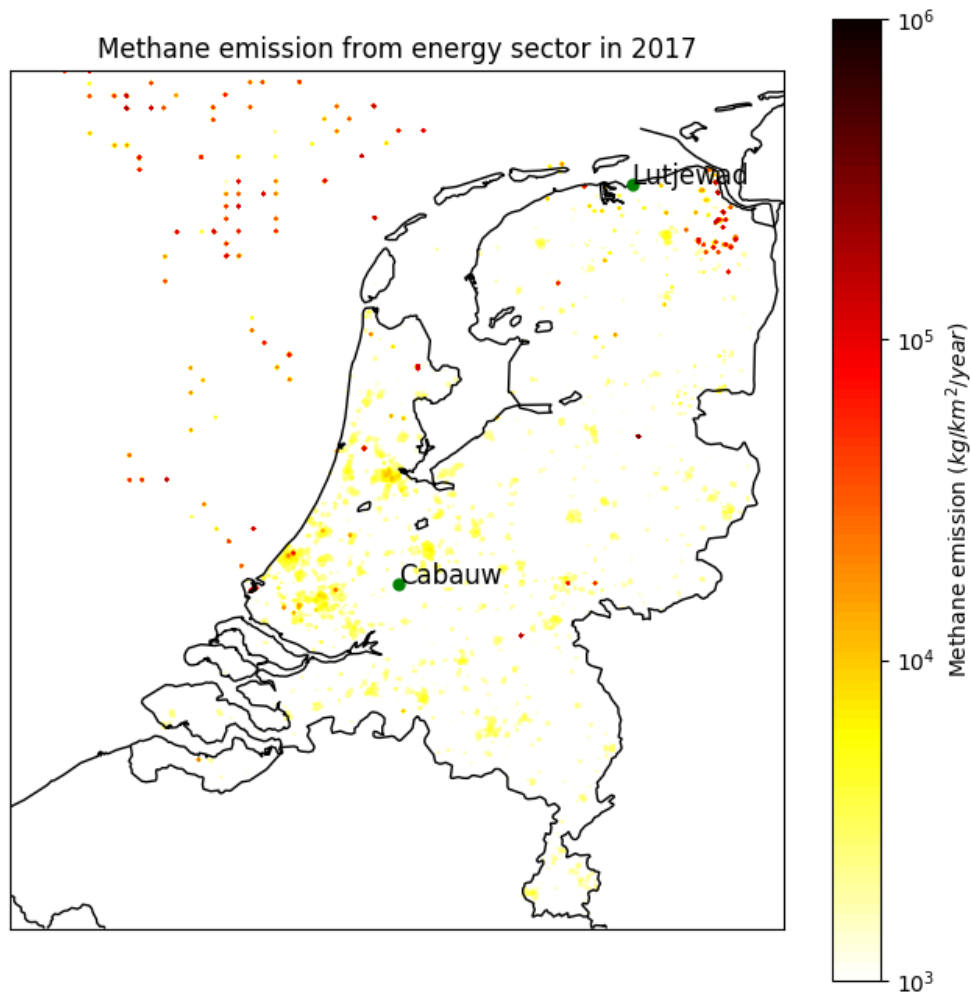


Figure 22: CH₄ emissions from the energy sector in the Netherlands in 2017. Note that emissions smaller than 10^3 kg/km²/year are not shown on the map.

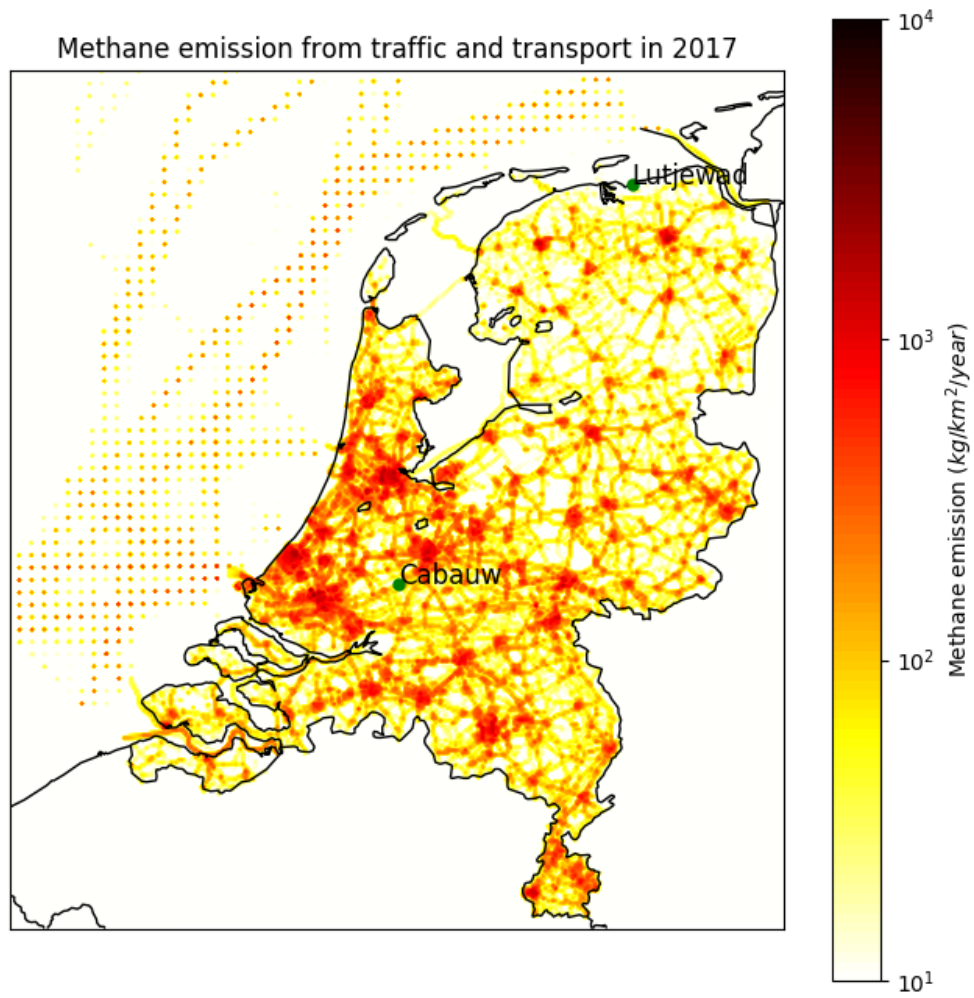


Figure 23: CH₄ emissions from the traffic and transport in the Netherlands in 2017. Note that emissions smaller than 10^1 kg/km²/year are not shown on the map.

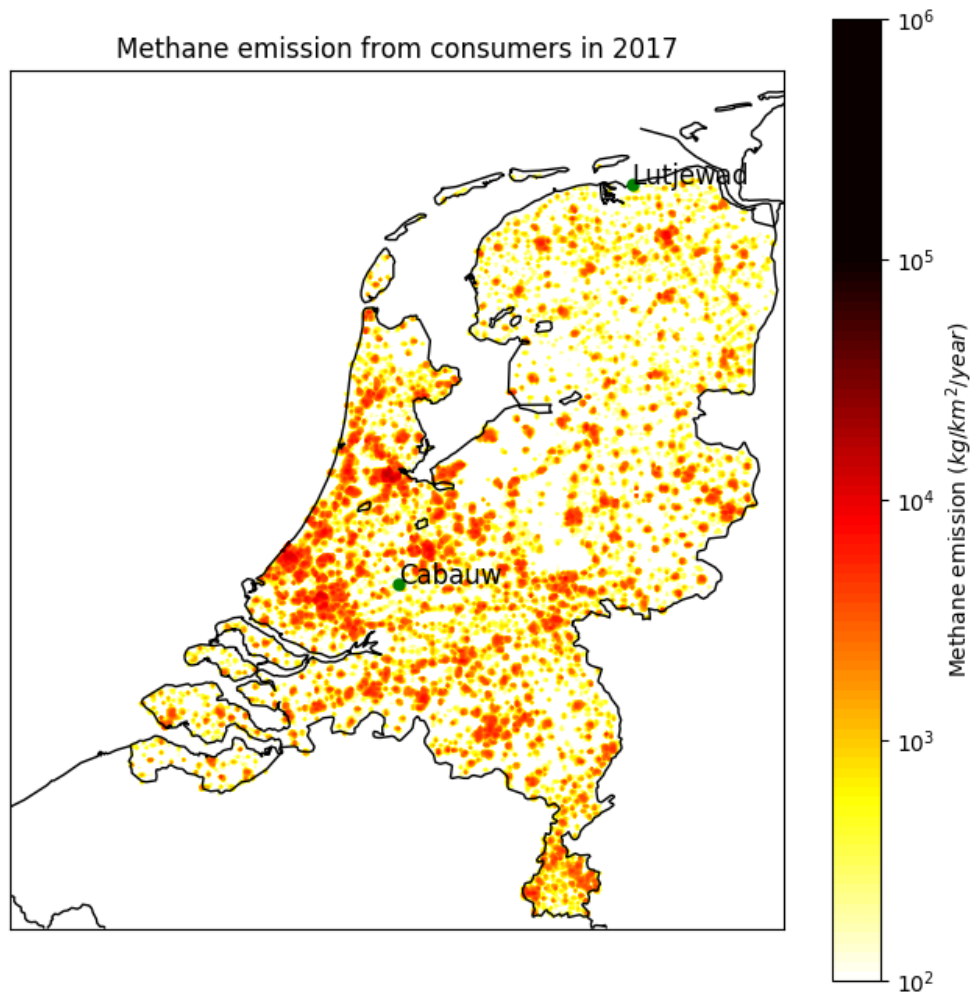


Figure 24: CH₄ emissions from the consumers in the Netherlands in 2017. Note that emissions smaller than 10² kg/km²/year are not shown on the map. Emissions above 10⁵ kg/km²/year are indicated with the color black.

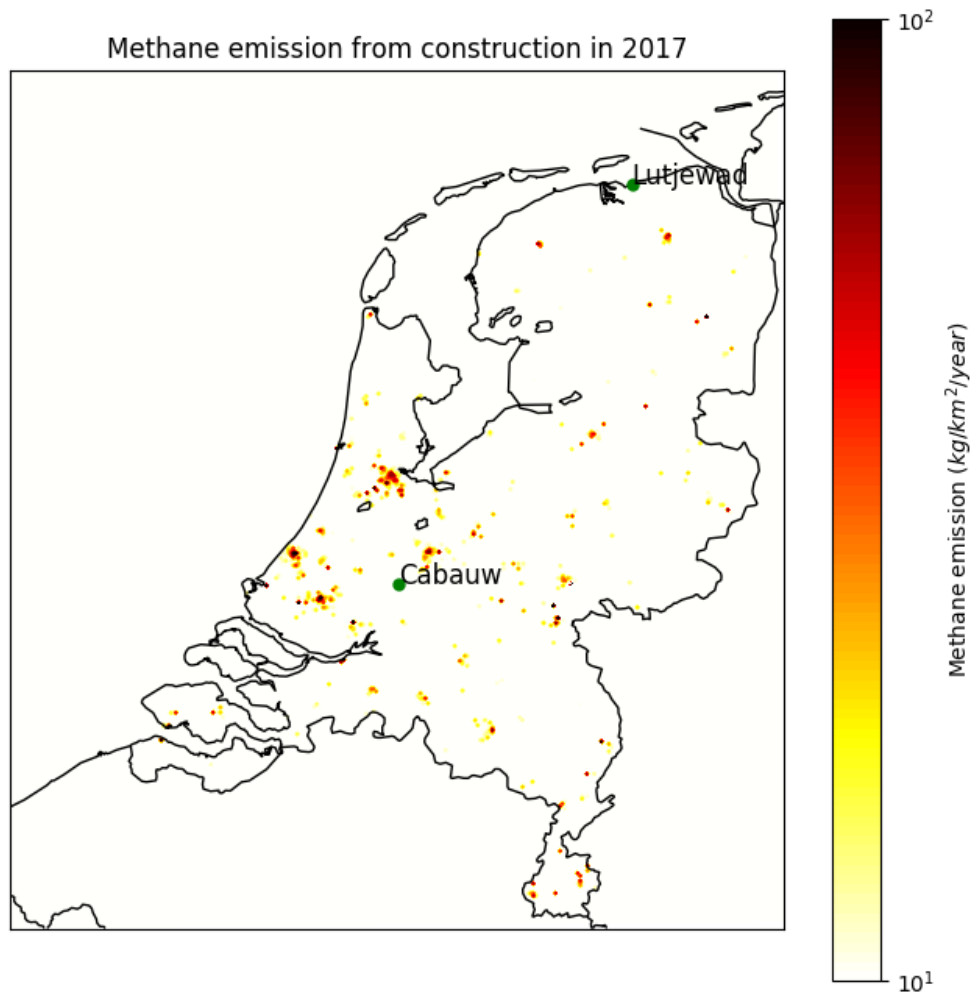


Figure 25: CH_4 emissions from the construction in the Netherlands in 2017. Note that only emissions between $10^1 \text{ kg}/\text{km}^2/\text{year}$ and $10^2 \text{ kg}/\text{km}^2/\text{year}$ are shown on the map.

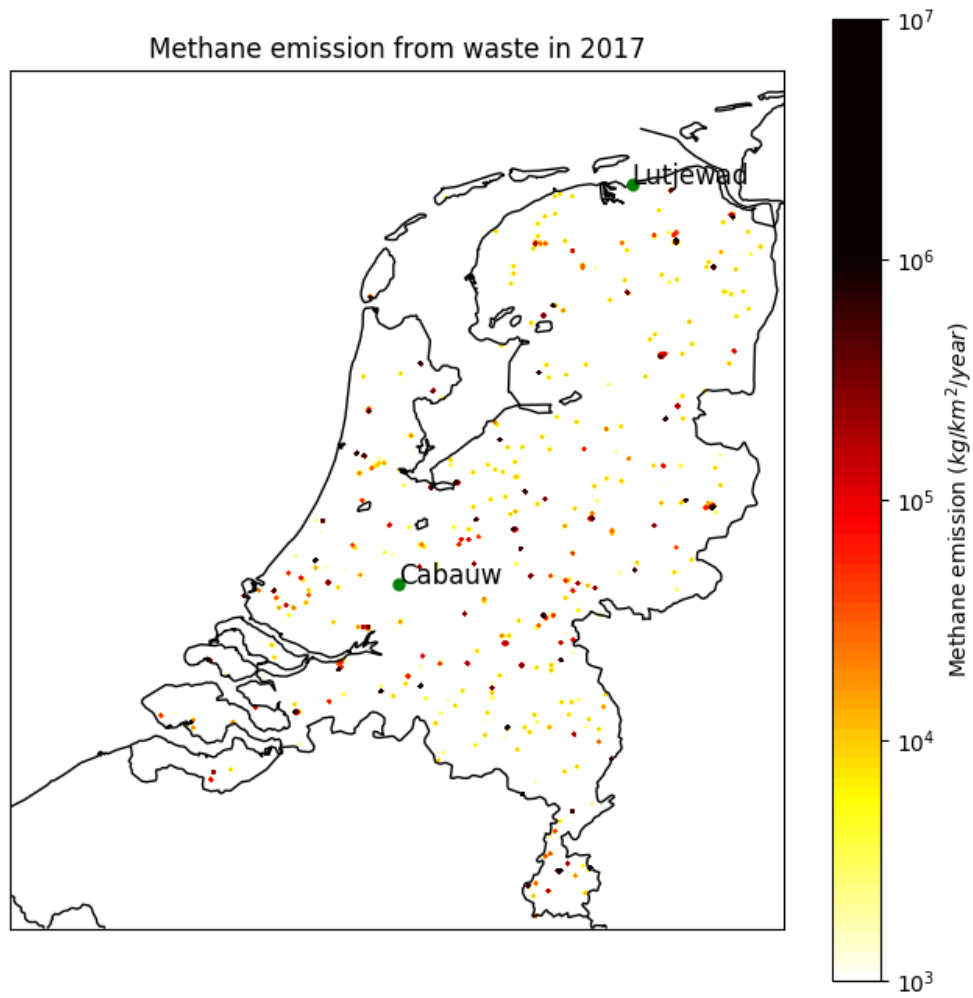


Figure 26: CH₄ emissions from the waste treatment in the Netherlands in 2017. Note that emissions smaller than 10³ kg/km²/year are not shown on the map. Emissions above 10⁶ kg/km²/year are indicated with the color black.

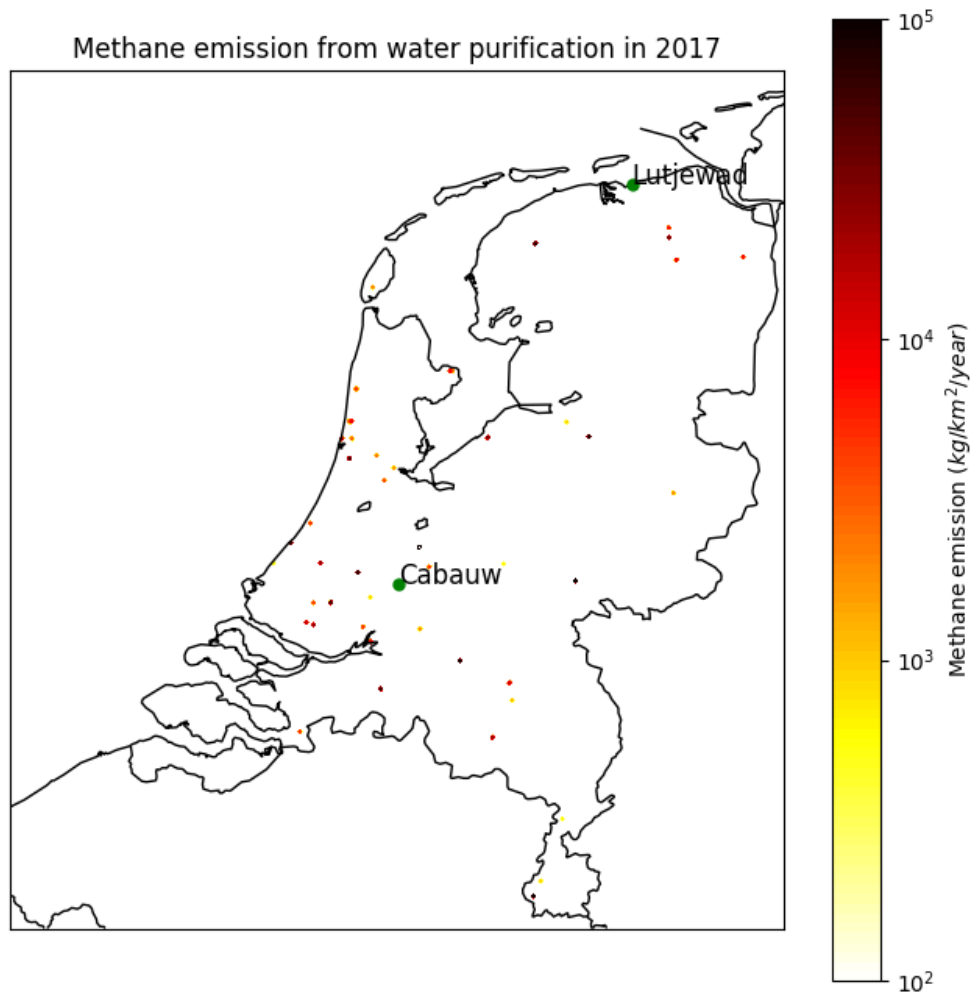


Figure 27: CH₄ emissions from the water purification in the Netherlands in 2017. Note that emissions smaller than 10² kg/km²/year are not shown on the map.

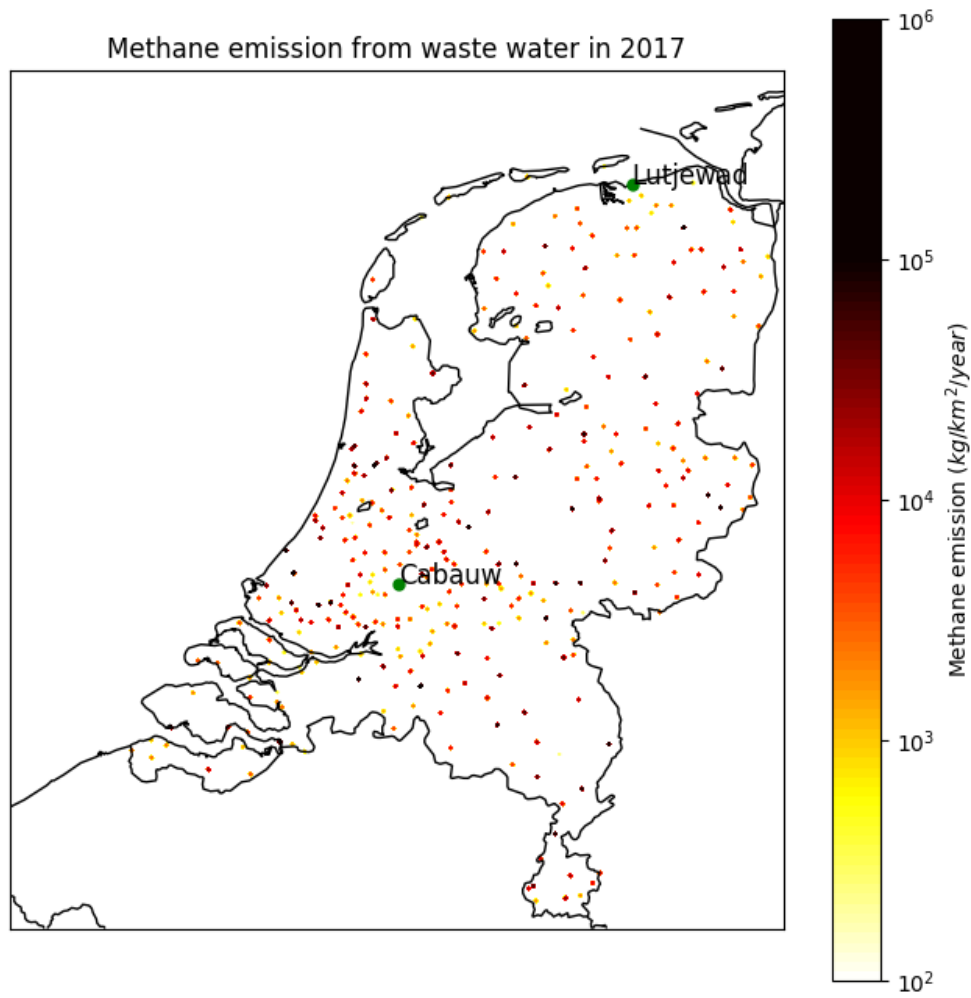


Figure 28: CH₄ emissions from the waste water in the Netherlands in 2017. Note that emissions smaller than 10² kg/km²/year are not shown on the map. Emissions above 10⁵ kg/km²/year are indicated with the color black.

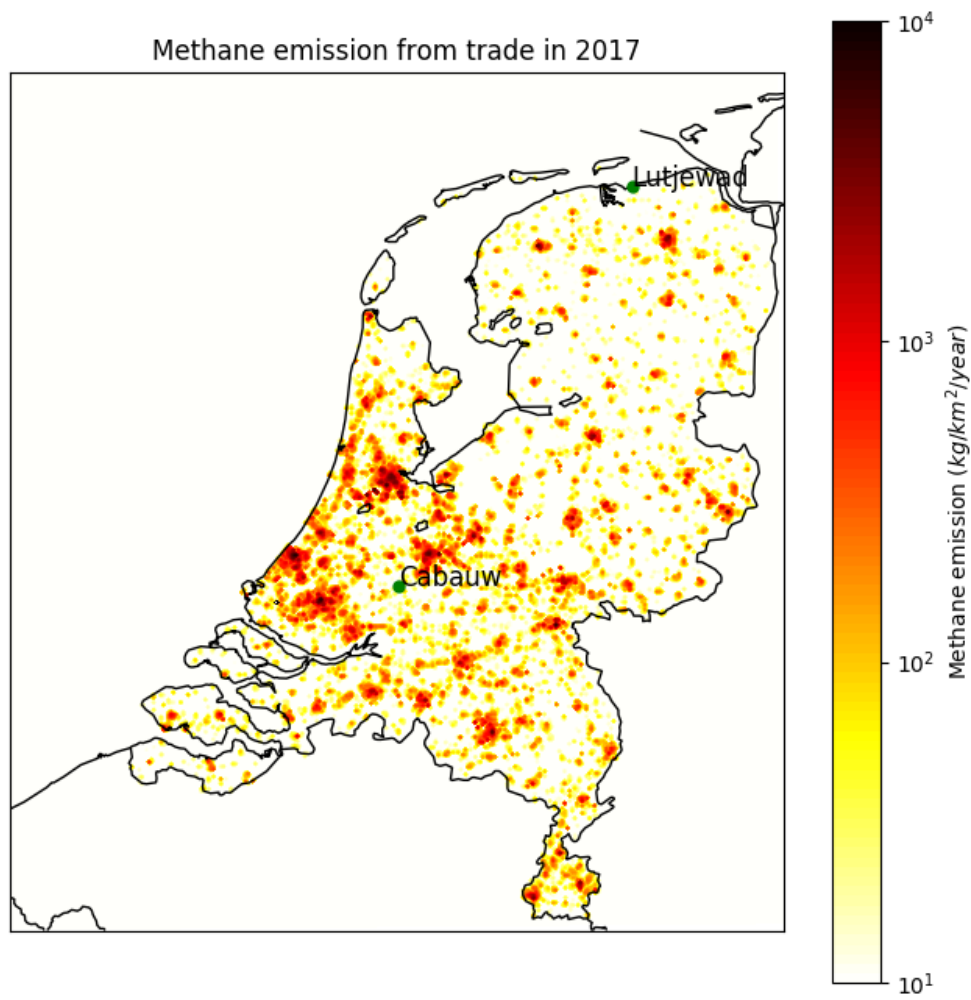


Figure 29: CH₄ emissions from the trade sector in the Netherlands in 2017. Note that emissions smaller than 10¹ kg/km²/year are not shown on the map.

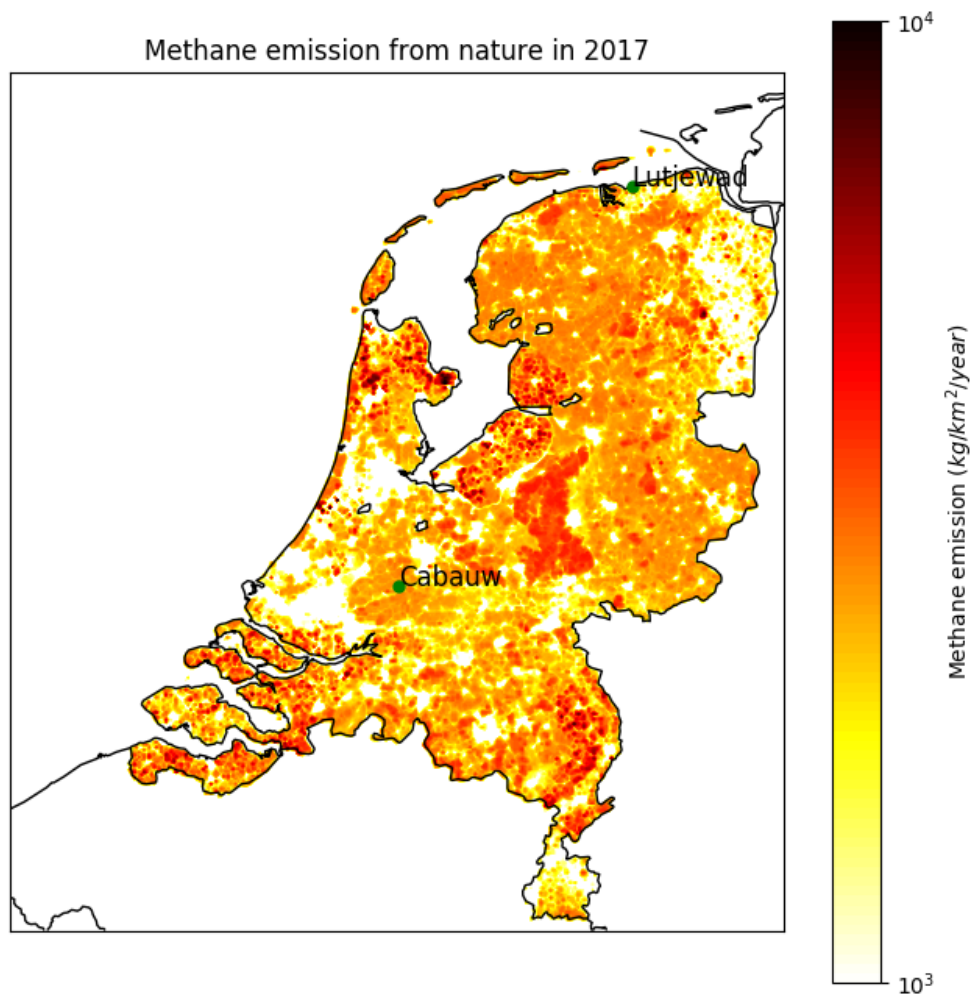


Figure 30: CH₄ emissions from the nature in the Netherlands in 2017. Note that only emissions between 10^3 kg/km²/year and 10^4 kg/km²/year are shown on the map.

7.3 WRF namelist settings

WPS-namelist settings

```
&share
wrf_core = 'ARW',
max_dom = 2,
start_date = '2017-01-01_00:00:00','2017-01-01_00:00:00','2017-01-01_00:00:00',
end_date   = '2017-12-31_18:00:00','2017-12-31_18:00:00','2017-01-31_18:00:00',
interval_seconds = 21600,
io_form_geogrid = 2,
debug_level = 0,
/

&geogrid
parent_id      = 1,1,2,3,
parent_grid_ratio = 1,3,3,
i_parent_start  = 1,36,45,2,
j_parent_start  = 1,32,57,2,
e_we           = 100,88,16,
e_sn           = 100,112,16,
geog_data_res  = '2m','30s','30s','30s',
dx = 9000,
dy = 9000,
map_proj = 'lambert',
ref_lat  = 52.2,
ref_lon  = 5.2,
truelat1 = 52.2,
truelat2 = 52.2,
stand_lon = 5.2,
geog_data_path = '/scratch/shared/freum/ivo/geog'
! ref_x = 50,
! ref_y = 46.5,
/

&ungrib
out_format = 'WPS',
prefix = 'FILE',
/

&metgrid
io_form_metgrid = 2,
fg_name = 'FILE'
/
```

WRF-namelist settings

```
&time_control
  run_days = 0
  run_hours = 0
  run_minutes = 0
  run_seconds = 0
  start_year = 2017, 2017, 2017, 2017
  start_month = 01, 01, 01, 01
  start_day = 1, 1, 1, 1
  start_hour = 0, 0, 0, 0
  start_minute = 0, 0, 0, 0
  start_second = 0, 0, 0, 0
  end_year = 2017, 2017, 2017, 2017
  end_month = 12, 12, 12, 12
  end_day = 31 31, 31, 31
  end_hour = 18, 18, 18, 18
  end_minute = 0, 0, 0, 0
  end_second = 0, 0, 0, 0
  interval_seconds = 21600
  input_from_file = .true., .true., .true., .true.
  history_interval = 60, 60, 60, 60
  frames_per_outfile = 24, 24, 24, 24
  history_outname = '/scratch-shared/ivoquax/WRF_Output/wrfout_d<domain>_<date>'
  adjust_output_times = .true.
  restart = .True.
  restart_interval = 1440
  io_form_history = 2
  io_form_restart = 2
  io_form_input = 2
  io_form_boundary = 2
  io_form_auxinput5 = 2
  auxinput5_interval_m = 60, 60, 60, 60
  frames_per_auxinput5 = 1
  auxinput5_inname = "wrfchemi_<hour>_d<domain_id>"
  write_hist_at_0h_rst = .true.
  ignore_iofields_warning = .false.
  debug_level = 0
/

&domains
  time_step = 27
  time_step_fract_num = 0
  time_step_fract_den = 1
  max_dom = 2
  e_we = 100,88,16,
  e_sn = 100,112,16,
  e_vert = 40, 40, 40, 40
  grid_id = 1, 2, 3, 4
```

```

parent_id = 1, 1, 2, 3
parent_grid_ratio = 1, 3, 3, 3
parent_time_step_ratio = 1, 3, 3, 3
i_parent_start = 1,36,45,2,
j_parent_start = 1,32,57,2,
dx = 9000,3000,3000,36000,
dy = 9000,3000,3000,36000,
p_top_requested = 5000
num_metgrid_levels = 61
num_metgrid_soil_levels = 4
feedback = 1
smooth_option = 0
/

&physics
mp_physics = 4, 4, 4, 4
progn = 0, 0, 0, 0
naer = 1000000000.0
ra_lw_physics = 4, 4, 4, 4
ra_sw_physics = 4, 4, 4, 4
radt = 30, 30, 30, 30
sf_sfclay_physics = 1, 1, 1, 1
sf_surface_physics = 2, 2, 2, 2
bl_pbl_physics = 1, 1, 1, 1
bldt = 0, 0, 0, 0
cu_physics = 3, 3, 3, 0
cudt = 0, 0, 0, 0
isfflx = 1
icloud = 1
surface_input_source = 1
num_soil_layers = 4
num_land_cat = 21
sf_urban_physics = 1, 1, 1, 1
maxiens = 1
maxens = 3
maxens2 = 3
maxens3 = 16
ensdim = 144
mp_zero_out = 2
mp_zero_out_thresh = 1e-08
cu_rad_feedback = .true., .true., .true., .false.
cu_diag = 1, 1, 1, 0
/

&fdda
grid_fdda = 2, 2, 0, 0
gfdda_inname = 'wrffdda_d<domain>'
gfdda_interval_m = 360, 360, 360, 360
gfdda_end_h = 8760, 8760, 8760, 8760
io_form_gfdda = 2
fgdt = 0, 0, 0, 0
if_no_pbl_nudging_uv = 1, 1, 1, 1
if_no_pbl_nudging_t = 1, 1, 1, 1

```

```

if_no_pbl_nudging_q = 1, 1, 1, 1
if_no_pbl_nudging_ph = 1, 1, 1, 1
ktrop = 0
guv = 0.0003, 0.0003, 0, 0
gt = 0.0003, 0.0003, 0, 0
gph = 0, 0, 0, 0
gq = 0, 0, 0, 0
xwavenum = 2, 0, 0, 0
ywavenum = 2, 0, 0, 0
if_ramping = 0
/

&dynamics
w_damping = 1
diff_opt = 1, 1, 1, 1
km_opt = 4, 4, 4, 4
diff_6th_opt = 2, 2, 2, 2
diff_6th_factor = 0.12, 0.12, 0.12, 0.12
base_temp = 290.0
damp_opt = 3
zdamp = 5000.0, 5000.0, 5000.0, 5000.0
dampcoef = 0.2, 0.2, 0.2, 0.2
khdif = 0, 0, 0, 0
kvdif = 0, 0, 0, 0
non_hydrostatic = .true., .true., .true., .true.
moist_adv_opt = 2, 2, 2, 2
scalar_adv_opt = 2, 2, 2, 2
chem_adv_opt = 2, 2, 2, 2
tke_adv_opt = 2, 2, 2, 2
/

&bdy_control
spec_bdy_width = 5
spec_zone = 1
relax_zone = 4
specified = .true., .false., .false., .false.
nested = .false., .true., .true., .false.
/

&grib2
/

&chem
kemit = 1
chem_opt = 17, 17, 17, 17
photdt = 30, 30, 30, 30
chemdt = 2.0, 2.0, 2.0, 2.0
io_style_emissions = 1
emiss_inpt_opt = 16, 16, 16, 16
emiss_opt = 17, 17, 17, 17
chem_in_opt = 0, 0, 0, 0
phot_opt = 1, 1, 1, 1

```

```

gas_drydep_opt = 0, 0, 0, 0
aer_drydep_opt = 0, 0, 0, 0
bio_emiss_opt = 0, 0, 0, 0
dust_opt = 0
dmsemis_opt = 0
seas_opt = 0
gas_bc_opt = 0, 0, 0, 0
gas_ic_opt = 0, 0, 0, 0
aer_bc_opt = 0, 0, 0, 0
aer_ic_opt = 0, 0, 0, 0
gaschem_onoff = 0, 0, 0, 0
aerchem_onoff = 0, 0, 0, 0
wetscav_onoff = 0, 0, 0, 0
cldchem_onoff = 0, 0, 0, 0
vertmix_onoff = 1, 1, 1, 1
chem_conv_tr = 1, 1, 1, 0
biomass_burn_opt = 0, 0, 0, 0
plumerisefire_frq = 0, 0, 0, 0
aer_ra_feedback = 0, 0, 0, 0
have_bcs_chem = .true., .true., .true., .true.
have_bcs_tracer = .true., .true., .true., .true.
vprm_opt = 'VPRM_table_EUROPE', 'VPRM_table_EUROPE', 'VPRM_table_EUROPE',
           'VPRM_table_EUROPE'
/

&namelist_quilt
/

```